Chapter 6
Some Aspects of Applying the Acoustic Emission Method

The direct industrial application of AE as a method of non-destructive testing of the integrity of structures and their elements, under periodic testing or in service conditions, is conditioned by the necessity to overcome a number of serious difficulties that arise due to the presence of significant industrial noise; the considerable loss of information during the passage of acoustic waves through large-scale structures; solving the problem of using multi-channel equipment to locate the defects in large objects; developing effective algorithms of the AE sources' location and data processing for every type of structure of a very complicated geometrical shape and welded and other types of joints, etc. Besides, malfunctions of a device often occur during long-term experiments or NDT. Thus, for example, there is no reliable AET that can be used in aggressive environments, at elevated temperatures and pressure, at vibration, etc. Therefore, the structure of such an AET requires additional technical improvements concerning the operating conditions and service lifespan. It is necessary to develop high-speed and reliable facilities for processing the information recorded by AET and presenting the results, which would enable reducing the extra staff engaged in operating these systems of AE testing.

These difficulties are basically related to the lack of reliable data on the nature of crack propagation under various loading conditions in aggressive environments. Despite the above-mentioned difficulties, the data on the practical application of the AE method accumulated so far, clearly indicate that this type of non-destructive testing permits detecting and evaluating the location, and the stages of sub-critical crack growth in large-scale structures operating in industrial conditions.

Z. Nazarchuk et al., *Acoustic Emission*, Foundations of Engineering Mechanics,
DOI 10.1007/978-3-319-49350-3_6

6.1 Specific Features of Long-Term AE Testing of Industrial Objects

The AE signals caused by crack propagation in metals can be subdivided into two types [1]. The first represents a continuous emission and is conditioned by an avalanche motion of dislocations and the formation of stable micro-cracks in the process of the development of plastic zones. The second is discrete AE caused by the crack front advance in the PZ, and by coalescence of micropores in the crack tip area.

In general, while testing large-scale structures by the AE method, due to considerable damping of signals it is necessary to record the AES caused by the crack front movement. At sub-critical crack growth, these signals usually have the form of short pulses of considerable amplitude. They are emitted for a certain time when the crack front propagates, and then, for several days or sometimes weeks, the AE can be very slight or even absent. The average value of periods of low activity of the AE usually decreases with an increase of the stress state.

On this account, the AE testing of the investigated objects should be carried out over a long period of time; in this way, a great amount of information is gathered. This means that the AE testing system should have a large information capacity. It should also be capable of selecting and quantitatively processing the information related to the relatively short periods of a crack growth that include the AE data obtained during the test time—which can last several weeks or months. In such systems, it is also necessary to foresee the possibility of accounting the parameters of aggressive environments and other features of a technological process that urge the crack initiation and propagation.

6.1.1 Selection of a Frequency Band and AET Placing

The AES spectrum, caused by individual crack jumps at the rate of several thousand meters per second over short intervals, is rather wide and comprises a region of high frequencies. However, while moving away from the source, high-frequency components decay much more than low-frequency ones. A similar type of decaying is observed for different mechanical noises; therefore, the band of working frequencies should be appropriately chosen to maximally increase the distances at which the defects could be detected and, at the same time, to minimize the noise level by increasing the recorded frequency band. The AE system, which consists of a resonance AET and a corresponding preamplifier with a band filter that has a sensitivity maximum at a frequency of 200 kHz with the pass band within the range of 200 kHz [2], is most suitable for practical application, except for the cases in which the noise level is extremely high.

To obtain the necessary sensitivity and the maximum tested area of a structure with a minimum number of AET, it is necessary to carry out the following investigations:

1. Study the statistical distribution of the AES amplitudes near the sources for each material and fracture mechanism. Since a crack often nucleates in the welded joints, it is necessary to perform experiments on specimens with welded joints, choosing the loading conditions and service environments close to real operating conditions.
2. Investigate the character of generation of the mechanical noises caused by the operating equipment, turbulent liquid flows, and friction, as well as other technological reasons by their dependence on the conditions of structure operation.
3. Carry out experiments on the evaluation of sound dispersion in the investigated object, especially during elastic wave propagation along a weld, and at the presence of screening effects conditioned by geometrical features of a structure.
4. Establish the level of electric noises in the measuring system, as well as transitional properties of vibrations transmitted by signals from the AET to the AE testing system, in order to minimize the loss of a signal and provide a reliable screening against electromagnetic industrial noise.

The level of mechanical noises determines the threshold level during AES recording, which together with estimation of the damping value of signals in all important directions, determines the maximum distance from the AE source to the AET, which is capable of detecting the propagating defects. This determines the minimum density of AET allocation on the surface of IO.

During crack growth in welded joints of large-scale steel structures, the AES amplitudes lie mainly in the range of 70… 80 dB with respect to the level of 1 μV, on condition that measurements are done at the standard distance of 20 cm from the source. The AET sensitivity is 67 dB (with respect to the level of 1 V/μBar at a frequency of 200 kHz). In such a case, at the threshold level of 26 dB, the detection distance of a fatigue crack attains 3 m at the initial stages of its growth in various joints that are on an off-shore platform in extreme weather conditions.

Figure 6.1 shows the dependence of the amplitude of AES radiated by a fatigue crack and by a calibrating generator on the distance between the AE source and AET. A generator of pulses with an amplitude of 10 V was used to evaluate the damping of the AES amplitudes. Proceeding from this figure, a maximal possible distance between the AET of AES is determined, using the dependences between sensitivity of the channel of the receiving system, sound attenuation, and the selected threshold level.

In order to unambiguously determine and locate the AE source, only four AETs capable of recording signals from this source are required. In this case, four AET were placed in such a way that the greatest distance from the AE source inside the controlled region of a structure to the receiver did not exceed 5 m.

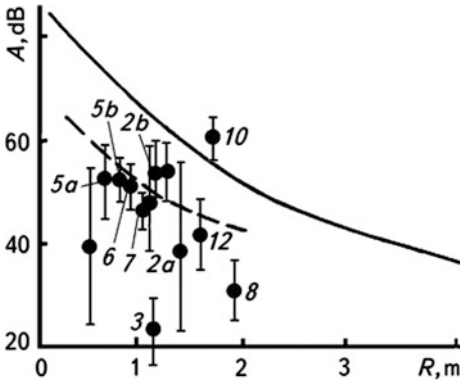

Fig. 6.1 Dependence of the AES amplitudes A on the distance R between the source of radiation and AET for different types of the AE sources: calibrating generator (*solid line*), fracture of a graphite rod (*dotted line*) and a fatigue crack (*dots with the indicated interval of amplitude variation*)

When the mechanical noise level changes, the threshold level should also change automatically; otherwise, the data recording by the AE testing system will stop at moments of a considerable increase of technological noises.

6.1.2 Calibration of an AE Testing System

The sensitivity of every AET after being mounted on the IO surface could be evaluated using the measurement results of the AES recorded by AET during the progress of an impact-simulated wave. The European working group on AE [3] recommended using the fracture of a pencil lead as an impact wave source located at a distance of 10 cm from the receiving AET center. The parameters of a pencil lead should be as follows: hardness—2H; length—3 mm; diameter—0.5 mm. Typical results of such experiments are shown in Fig. 6.1. Every group of AET located on the structure should make it possible to locate such AE source at any point of the structure region inspected by this group of the AET. At durable AE testings of structures and objects of different types—except for the calibration procedure described above—a generator of ultrasonic vibrations is used that is turned on either automatically or manually, and which is used for periodic verification of service capability of the equipment channels and their sensitivity [4].

6.1.3 Analysis and Presentation of AE Test Results

Specific types and mechanisms of fracture typical of these structures, as well as possible fields of application of the test results, require an appropriate analysis and specific methods of processing and presenting the results of durable AE testing of various structures.

It is well known that sub-critical fatigue crack growth is a slow process that requires durable observations to obtain reliable information on a defect growth. The

average time between incremental steps of a crack propagation as well as the causes of the crack appearance, are important characteristics of a fracture. Furthermore, information on the stress state and the parameters of service environment, such as temperature, pressure, vibrations that arise during the operation of a structure, and because of friction, are very important for the evaluation of susceptibility of structures to the initiation and propagation of defects.

High density of the difference of the AES arrival times can be used as one of the most reliable AE parameters of—crack growth. In the case of locating four AET, the values of the difference of the AES arrival times are relative moments of time during which the signals from a source reach each AET, which is evaluated with respect to the time of a signal arrival to the first AET. Since the AET and the source positions are fixed, certain differences of the arrival time will contain a bias error that depends both on the transmission function of the environment through which an elastic wave propagates, and on the direction and distance of propagation, the AET type, and the method of mounting it on the IO.

As described in paper [5], the values of the differences of arrival times for densely localized sources that generate repeated AES usually differed by not more than one micro-second at the distances from the source to the AET of about 6 m in the welded joints of pressure vessels and in other structures. It should be noted that this situation was observed, as a rule, during sub-critical crack growth.

Periods of a strong regular AE, the duration of which, in most cases, does not exceed a few minutes, (as mentioned above), are replaced by long periods (days or even weeks) of the AE of low activity. Since it is impossible to predict the moment of a crack growth start in real structures, the AE testing should be carried out over long periods. Therefore, it is important to summarize the results for a regular period —for example, for a week or a month—using a plot for data presentation similar, for instance, to that in Fig. 6.2. This figure represents fully enough the information necessary for evaluating the degree of a defect danger, namely:

- The sites of the AE sources that can serve as a measure of evaluation of the defect length in projections are shown;
- The density of the AE events that characterizes the depth of a defect location;
- The dependencies of the number of AE events on time that determine the crack growth rate; and
- The value of various technological parameters (for instance, temperature, pressure, and vibration) that enables forming conclusions on the causes of a crack.

6.1.4 Stability of AE Parameters

The AES contain information on the parameters of dynamic processes in a solid that are accompanied by an elastic wave radiation. Usually the following parameters of

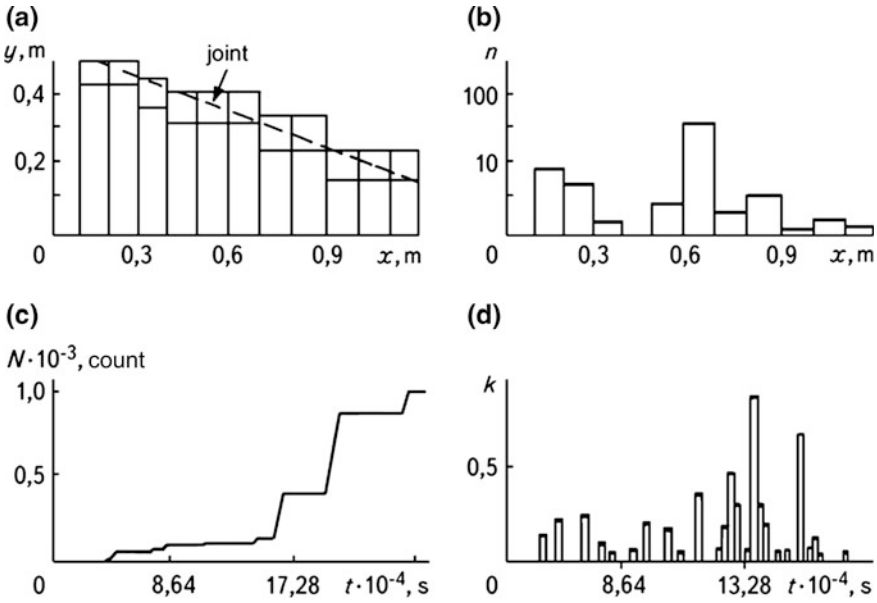

Fig. 6.2 Results of the AE testing of a weld: **a** is the graphic presentation of results of the AE location of a weld region; **b** is the distribution of the number of AE events in different regions of the welded joint; **c** is the time dependence of the cumulative AE count N; and **d** is the time dependence of the technological parameter

an AES are used: the number of recorded pulses; the rate of their count; energy and duration of pulses; duration of the forward and back fronts of a pulse; duration of the interval between pulses; frequency spectrum; the AE activity, etc.

When selecting a parameter or a group of AE parameters, one should take into consideration their relationship with the parameters of dynamic processes (e.g., a fracture process) that occur in a solid. Then, it is necessary to give advantage to those AE parameters that bear maximum information and are convenient for selection and processing, and are resistant to various factors that can affect these parameters.

During experiments with the AE application, as a rule, considerable data scattering is observed. To a great extent, this is related to the fact that the values of the recorded parameters depend on such factors as properties of the chosen AET, the distance from AET to the signal source, amplitude-frequency characteristics of the recording equipment, the threshold level chosen, properties and shape of the material, structural features of the investigated object, and so on. The effect of these factors on the recorded AE parameters is certainly unknown, which brings about considerable difficulties when comparing the results obtained in various conditions of the AES recording and interpreting them. Proceeding from the above-mentioned, an important problem to be solved while applying AE is establishing the stability of a particular parameter under the action of different sources of elastic wave generation.

As follows from [6], the effect of the threshold level on the AE parameters can be studied by changing this level within the signal amplitude range and by evaluating the AE parameters investigated. Within the experiment, simultaneously changing a threshold level and any other factor, for instance, the distance between the source and the AET, it is possible to evaluate their mutual effect.

The extent of stability of the AES parameters affected by a definite factor is determined as follows: Measurements of cumulative count, e.g., $N = km$ are carried out, where k is the number of the values of the investigated factor, e.g., the number of threshold levels. For each level of a factor $t = 1, 2, \ldots, k$, m measurements of the AE parameter X_{ti}, $i = 1, 2, \ldots, m$ are done. Thus, there are k groups with m measurements of parameters in each.

For every level of the factor, the average value of a parameter is calculated by the formula

$$X_t = \frac{1}{m}\sum_{i=1}^{m} X_{ti}. \tag{6.1}$$

Having averaged overall measurements, we get

$$X = \frac{1}{N}\sum_{t=1}^{k} mX_t. \tag{6.2}$$

Mean-square divergence of the average values of a parameter in a group from an overall average value is:

$$\sigma_1^2 = \frac{1}{k-1}\sum_{i=1}^{k} m(X_t - X)^2 \tag{6.3}$$

and mean-square divergence of a parameter from its average value in a group is:

$$\sigma_2^2 = \frac{1}{N-k}\sum_{t=1}^{k}\sum_{i=1}^{m} (X_{ti} - X_t)^2. \tag{6.4}$$

If the mean-square divergence between groups exceeds the mean-square of divergence in a group, this indicates that there is a real difference between the groups. The ratio of the mean-square divergences can be used for the quantitative estimation of this difference.

$$R = \sigma_1^2/\sigma_2^2. \tag{6.5}$$

To investigate the mutual effect of several factors, it is possible to introduce a measure similar to (6.5). The mean-square divergence for two factors is calculated

Table 6.1 Mean-square divergence of the parameter values for two factors

Source of changes	Mean-square divergence
First factor	$\frac{mc}{k-1}\sum_{i=1}^{k}(\bar{X}_i-\bar{X})^2$
Second factor	$\frac{mk}{c-1}\sum_{i=1}^{c}(\bar{X}_i-\bar{X})^2$
Interaction of factors	$\frac{m}{(k-1)(c-1)}\sum_{t=1}^{k}\sum_{i=1}^{c}(\bar{X}_{ti}-\bar{X}_t+\bar{X}_i+\bar{X})$

by the formulas presented in Table 6.1, where c is the number of levels of the second factor.

The relationship (6.5), as can be proved under some assumptions, has a non-central F-distribution with $(k-1)$ and $(m-k)$ degrees of freedom tabulated in [7]. As a verification criterion of the hypothesis on the general effect of a corresponding factor in case of accurately calculated level of significance, the ratio of R to the tabular value of F-distribution should be taken

$$R_F = R/F_{k-1;N-k;0.999}, \tag{6.6}$$

and, with a probability of 0.999, we should estimate whether the investigated factor affects the corresponding AE parameter. If $R_F > 1$, the effect of this factor on the respective AE parameter is observed, and the extent of its significance is proportional to R_F. Under the mutual action of several factors, the R_F value describes the variation of the effect of one of them on the AE parameters when the other factor is changed.

In order to evaluate the degree of stability of some AE parameters in the experiment, the distance of the AET from the AE source was changed. The recorded signals were processed at various threshold levels. A piezoelectric transducer, excited by a pulse electric signal, was used as a stable source of acoustic signals that permits receiving reproducible results. The experiment was carried out on a cylindrical pressure vessel 1600 mm high and 600 mm in diameter, with an 80 mm wall thickness made of shell 12X2NMFA steel. Signals were recorded by D9102 AET of a differential type produced by the Dunegan/Endevko Company. The overall amplification of the receiving channel was 80 dB. An amplified signal was recorded by a digital memory oscilloscope and then transmitted to a computer, where the AES parameters were determined. The AES were recorded by the sequential setting of a transducer on the investigated surface every 10 cm, and by conducting 4 measurements at each of its positions. Cumulative count N, maximum amplitude A, energy E, signal duration T, rise time T_r as well as signal propagation velocity v, were calculated from these data. The parameters mentioned were found for the AES recorded at the threshold levels that changed from 0.2 to 1 V with the step of 0.1 V.

Changes in the AE cumulative count depending on the distance to the AET at different threshold levels are shown in Fig. 6.3.

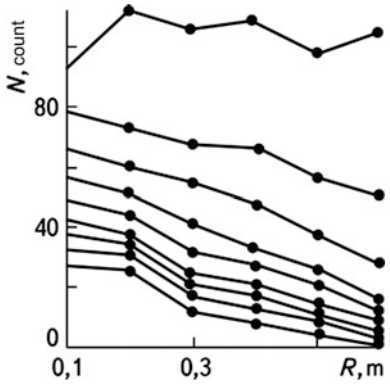

Fig. 6.3 Dependence of the AES cumulative count N on the distance R between the AE source and the AET at different values of a threshold level, which changed stepwise every 0.1 V starting from 0.2 (*upper curve*) to 1 V (*bottom curve*)

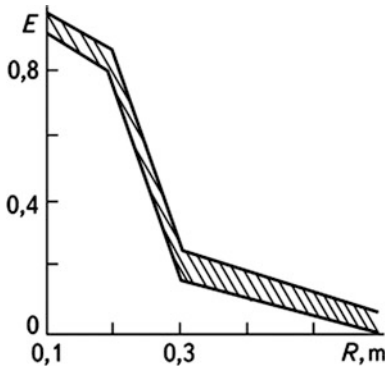

Fig. 6.4 Dependence of the AES E energy on distance R between the AE source and the AET at various threshold level values, which changed from 0.2 (upper boundary of the *shaded region*) to 1 V (lower boundary)

With an increase of the distance, the value of N decreases linearly, and the dependence on the threshold level is close to a logarithmic one. A signal duration changes in a similar way. It was measured as the time interval between the first and the last signal crossing the threshold level.

As seen in Fig. 6.4, a signal energy E dropped more sharply during an increase in the distance. However, it only slightly depended on the threshold level. Similarly, the AES amplitude A depends on the distance. Signal rise time T_r was determined, starting from the moment of signal crossing the threshold level until the moment of reaching the maximum amplitude.

The T_H versus threshold level dependence at various values of the distance from the AET is shown in Fig. 6.5. The velocity observed of the AES propagation was estimated as a relation of the distance between the source and the AET to the time of a signal arrival, recorded at the moment of its crossing the threshold level or at the moment of reaching the amplitude maximum $A_{\max}$. For all the signal parameters discussed above, the value of stability coefficient R_F, whose values are presented in Table 6.2, was calculated. It was found that the most unstable parameter with respect to the threshold level is a cumulative count, while the most stable is the signal energy.

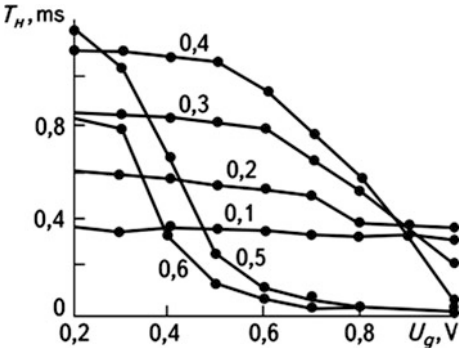

Fig. 6.5 Change in the AES rise time T_H during an increase of the threshold level Ug for distances R = 0.1; 0.2; …0.5 m from the AE source to the AET

Table 6.2 Stability coefficients R_F for the AES parameters in relation to the change of threshold level and a distance to the source

Factors of the change of stability coefficient	Parameters						
	N	I	E	A	τ	V_p	V_A
Threshold level	53	42	0.1	–	20	16	–
Distance between the AE source and AET	11	2.6	44	55	19	16	79
The interaction of two factors: the threshold level and the distance between the AE source and AET	0.6	1.3	0	–	4.8	2	2

As seen in Table 6.2, a relative stability of a parameter in regard to one of the considered factors is accompanied, as a rule, by a relative instability in regard to the other factor. The sum of stability coefficients tends to preserve to the threshold level and the distance. Stability coefficients for the interaction of factors are lower by about one order than the stability coefficients for each factor separately. Therefore, the order of the values of stability coefficients at interaction is preserved if one of the factors changes. Similarly, it is possible to determine the effect of other factors on the AES parameters, such as the band pass of equipment, the AET type, conditions of its mounting on the specimen surface, its shape, etc.

It was established that various AES parameters show different stability to a threshold level and a distance. Therefore, one should either choose the parameters with a maximum stability and use them as informative parameters of the AES during the AE testing of structures, or provide procedures to reach this stability.

6.1.5 Classification of AE Sources by Their Activity

Difficulties in using the AE as a method of non-destructive testing are mostly related to the absence of reliable criteria that make it possible to determine the risk

degree of the defects detected in the structure investigated. The state of an object is most often determined by the dependence of the cumulative count of AE on the SIF [8]. This approach is considered more generally in [9, 10], where, in particular, it is suggested to describe the dependence of the AE cumulative count on any loading parameter, e.g., load value, number of cycles, time, and so on, using a statistical dependence.

According to the classification proposed in [11], the AE sources are subdivided into three groups: C are non-active sources, for which the number of the AE events during observation increases only slightly; B are active sources, where the dependence of cumulative count on the applied load is relatively linear for them; and A are critically active sources, where the number of the AE pulses grows rapidly.

Sources classified as non-active are recorded, but they are not observed later on. Active sources need to be observed, while during the recording of a critically active source, it is recommended that a non-destructive testing be conducted using other methods.

Paper [12] proposes a system of classifying the AE sources used as a basis in a Japanese standard for testing spherical vessels [13]. Each AE source in this system refers to a certain class and type. The class of the source is determined by the total radiated energy and its density emitted from a unit of the source area, and the type of the source is determined by the dependence of total energy on the loading parameter. Four classes and four types of sources are examined in this system. On this basis, they are subdivided according to the degree of danger, into four groups: A, B, C, and D. Group A includes sources, the presence of which requires an immediate interruption of loading; Group B includes the sources whose localization region should be checked using traditional methods of non-destructive testing; and Groups C and D include the AE sources that are not dangerous and do not claim special attention.

The method belonging to the first group of the above-mentioned classification does not have any obvious criteria of structure scrapping, and is based on qualitative approaches that do not take into account a jump-like character of a fracture. The second method differs by a very complicated procedure of estimating the danger of defects, and there are no valid criteria of their classification.

Paper [10] formulated the problem of determining the numerical criteria of estimating the danger of AE sources using the AE test results based on the parameters of AES, which can be easily determined (for instance, the cumulative count of AE, which is related to amplitude and duration of the AE pulses, and, therefore, to the process energy). Since the AE is known to be a discrete process, the growth of cumulative count is also a stepwise function.

If the loading parameter increases by $\Delta\Pi$, then the cumulative count of AE increases by ΔN_i. By approximating two successive values of the Π_i and N_i quantities by power dependence

$$N_i = A_0 \Pi_i^{m_i}, \tag{6.7}$$

where A_0 is the proportionality factor, m_i is the power index. For ΔN_i from (6.7), we get

$$\Delta N_i = m_i A_0 \Pi_i^{m_{i-1}} \Delta \Pi_i. \tag{6.8}$$

From dependencies (6.7) and (6.8), we find the power index

$$m_i = \Delta N_i \Pi_i (\Delta \Pi_i N_i)^{-1}. \tag{6.9}$$

Relationship (6.9) permits determining a power index at any stage of an increment of the AE cumulative count. Classification of the AE sources can be performed by m values at each step of the N increase. If m *is* less than one unit, a cumulative count derivative diminishes, and the AE activity of the process for this source drops. Such a source can be classified as non-active for this growth of the parameter. For $m \approx 1$, the AE process develops with a permanent intensity. The corresponding source is active, and on condition that $1 < m < 6$, it is critically active, and when $m > 6$, it is catastrophically active. It is clear that the same source can be classified as non-active at low levels of a load, or as critical and possibly catastrophically active at high values of the applied load. Final classification can be made only after performing the AE research in a given range of the applied loads.

The analysis of an m variation shows that this random value has two areas that are characterized by various average values. This is evident by the dependence of a cumulative count of load in logarithmic coordinates. In the first area, the source can be characterized as non-active or active, while in the second, its activity is critical or even catastrophic.

If we represent the random value of m as a parameter of probability distribution and we take into account the presence of the two above-mentioned areas, it is necessary to find for each of them the distribution by different mean values of m. For this purpose, the following exponential dependencies were chosen:

$$M_1(m) = v_1 \exp(-v_1 m), \quad M_2(m) = v_2 \exp(-v_2 m), \tag{6.10}$$

where $v_1 = 0.99$, and $v_2 = 0.33$. The validity of the empiric distribution in the sample was checked by means of the Pearson fitting criterion. Then the value of k_1^2 for the first approximation is 11.57, and for the second—$k_2^2 = 11.95$. If the level of significance $\alpha = 0.05$ and the degrees of freedom are 6 and 11, the critical values of k_{kp}^2 for approximations (6.10) will be 12.6 and 19.7, respectively. The values of k_1^2 and k_2^2 that were obtained are smaller than the critical ones, so it is possible to consider, with the given probability, that the experimental data are described satisfactorily by the laws of distribution (6.10) with the parameters described above.

To perform an effective acoustic-emission testing, it is necessary to find such criteria whose usage in the dependencies (6.10) permits estimating the degree of the

AE source danger for a structure. The selection of one of the two statistical hypotheses that determines to which type of distribution (6.10) the value of m belongs can be performed by successive procedures [14]. However, for a successive analysis, it is necessary that the distribution in the investigated sample be invariable; this criterion is not satisfied in the given case, because one stage of the cumulative count growth is substituted by the other one at the a priori unknown moment. Therefore, the investigated samples will be mixed up. In this connection, it is necessary to have a criterion that permits distinguishing the second stage of an increase of the AE cumulative count. If the criterion is satisfied, then it is possible to check a hypothesis on the validity of the second distribution (6.10) because it corresponds to the critical and catastrophically active AE sources.

A successive procedure for such estimation is as follows [7]: Some threshold value m_{th} of m is assigned—hardly probable for the first area, and highly probable for the second. In such cases, after a sequence of independent experiments in which realization of the event E_0 in each of them is checked, and which consists of m exceeding the given threshold value, it is possible to get two expressions for a number of experiments, where the event E_0 took place:

$$\begin{aligned} Z_{k1} &= \frac{\ln[\alpha_0/(1-\alpha_1)] + k\ln[(1-p_1)(1-p_0)]}{\ln[p_1(1-p_0)/p_0(1-p_1)]}, \\ Z_{k2} &= \frac{\ln[(1-\alpha_0)/\alpha_1] + k\ln[(1-p_1)(1-p_0)]}{\ln[p_0(1-p_1)/p_1(1-p_0)]}, \end{aligned} \tag{6.11}$$

where α_0 and α_1 are the assigned probability of errors of the hypothesis H_0 on the validity of the second distribution (6.10) and an alternative hypothesis H_1, respectively, p_0 and p_1, are the conditional probability of the event E_0 when the hypothesis H_0 and an alternative hypothesis H_1 are valid, respectively.

$$\begin{aligned} p_0(m \geq m_{\text{th}}/M_2) &= \int_{m_{\text{th}}}^{\infty} M_2(m)\mathrm{d}m, \\ p_1(m \geq m_{\text{th}}/M_1) &= \int_{m_{\text{th}}}^{\infty} M_1(m)\mathrm{d}m. \end{aligned} \tag{6.12}$$

In the coordinates, k is the number of experiments, Z_k is the number of the events E_0, and there are three regions, divided by parallel lines for the successive procedure (6.11).

It follows from the analysis of the m value dependence that a hardly probable value of $m = 4$ for the first stage of fracture appears quite frequently at the second stage. Therefore, putting $m = 4$ (6.12) with the account of (6.10), we get $p_0 = 0.27$, $p_1 = 0.02$. The probability value of the error of the first kind α_0 (probability of an active source missing) should be assigned to be smaller than for the probability of the error of the second kind α_1, i.e., over-rejection. Proceeding from this, we can put

$\alpha_0 = 0.01$, and $\alpha_1 = 0.05$. If for the given p_0, p_1, α_0, α_1, the point (k, Z_k) is located above the region bound by two lines (6.12), it is assumed that the corresponding source can be classified as critical or catastrophically active.

The analysis [10] of the experimental data obtained for specimens made of the pressure vessel material showed that the point (k, Z_k) was as a rule outside the bound area for the third or fourth event E_0. With this conclusion, we can set forth other criteria that follow directly from the dependence of the AE cumulative count on a load.

Such criteria can be formulated as follows:

Putting in the relationship (6.7) as above, $m = m_{\text{th}} = 4$, we get

$$N_i = A_0 \Pi_i^4. \tag{6.13}$$

Then, the increment of the AE cumulative count will be

$$\Delta N_i = 4A_0 \Pi_i^3 \Delta \Pi_i. \tag{6.14}$$

Assuming that

$$\Delta N_{i+1} = 4A_0(\Pi_i + \Delta \Pi_{i+1}), \tag{6.15}$$

and taking into account that

$$N_{i+1} = N_i + \Delta N_{i+1}, \tag{6.16}$$

then it is possible to take the ratio of (6.15)–(6.13) as a criterion

$$\frac{\Delta N_{i+1}}{\Delta N_i} > \left(1 + \frac{\Delta \Pi_{i+1}}{\Pi_i}\right)^3 \frac{\Delta \Pi_{i+1}}{\Pi_i}. \tag{6.17}$$

When this inequality is satisfied, then $m > 4$.

During an accelerated growth of a crack, frequent increments of N occur, and the intervals of the loading parameter in this case are considered to be approximately the same and small $(\Delta \Pi_{i+1} \approx \Delta \Pi)$. Then, neglecting in (6.17) the higher order term of smallness, it is possible to get the following criterion:

$$\Delta N_{i+1}/\Delta N_i > 1 + 3\Delta \Pi_{i+1}/\Pi_i. \tag{6.18}$$

However, at the initial stages of loading at large values of $\Delta \Pi$, these criteria do not always correctly characterize the AE source activity. A more exact relationship can be obtained from (6.13) with the account of (6.16)

$$\Delta N_{i+1}/N_i > (1 + \Delta \Pi_{i+1}/\Pi_i)^4 - 1. \tag{6.19}$$

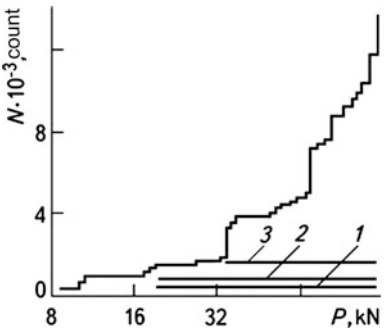

Fig. 6.6 Change in the cumulative count of AES N with load P for a 15X1M1F steel specimen with a notch under bending testing. *Straight lines* show the range of fulfillment of criteria (6.17), (6.18), and (6.19), respectively

Taking into account that power index m is a random value, the realization of criteria (6.17–6.19) is also a random event similar to the event E_0. The evaluation with a given degree of reliability can be performed by setting additional conditions that determine how many times the criteria should be satisfied. Similar to a successive evaluation, we can require satisfying the (6.19) three times. Hence, a given source should be considered a dangerous one for this structure. As is seen in Fig. 6.6, the criteria (6.17 and 6.18) are satisfied starting from the initial stage of fracture, and the criterion (6.19) is satisfied at the stage of accelerated crack growth. Thus, this criterion more reliably presents the degree of danger of the recorded AE sources. The obtained relationships (6.17–6.19) permit distinguishing the catastrophic stage of fracture, and together with the results of statistical analysis serve as decision-making criteria on the degree of the AE source danger for a structure.

6.2 Using the AE Methods for Testing the Offshore Platforms

For various technical and economic reasons, it is nearly impossible to perform an overall inspection of all kinds of units and joints of the offshore platforms. However, it is possible to check the individual parts that are most sensitive to crack initiation and propagation. A special AE testing system [1, 2] has been developed for this purpose. It consists of 4 × 32 channels and is equipped with 144 AET. The system permits checking various service parameters and all major units, welded joints, and places of fastenings that are on a platform.

The present system of the AE testing has the following characteristics:

- High sensitivity and low level of natural noises;
- Capability of choosing the working frequency range to get an optimum signal/noise ratio under a minimum effect of electromagnetic background (the average value of noises after treatment by the AES processor does not exceed one event per second);

- Distances at which it is possible to reveal the AES of small amplitude that are generated at early stages of crack formation in service conditions are 5…6 m;
- Reliable protection against atmospheric and mechanical damage;
- A specially protected and screened cable for transmission of high-frequency signals of low amplitude at a distance of more than 300 m at a minimum level of induction of electromagnetic hindrances;
- Rapid processing and assessment of the importance of the recorded AES;
- Possibility to take into account the external parameters (in the case of off-shore platforms these are accelerations, rotations, keel swaying, slope angles and height of waves, speed of wind, etc.) in order to predict the danger of the defects more exactly;
- Automatic calibration of the AET and the measuring paths as well as automatic checking of the obtained results; and
- A turn-off system acting in case a defect is located, and as a result the first four AETs of the six that recorded the AES are chosen, ensuring the best calculation of the defect localization.

In this case, for testing the off-shore platforms, the threshold level was selected to be equal to 26 dB (0 dB corresponds to 1 μV, and 120 dB—to 1 V). Sensitivity of the D9203AH AET was 67 dB in the pass band of 100…300 kHz. At this threshold level, the maximum speed of the recorded events was about 100 events per second.

The results of underwater testing of platforms [5] showed that the frequencies of 80 and 240 kHz were most expedient for the reduction of noise. The same frequencies provide a maximal increase of distances at which the AES recording is possible. Above 80 kHz, as the experiments showed, mechanical noise became considerably weaker, but the noise in water was at a very high level that could be reduced further by placing the AET in specially designed protective shrouds. Measurements conducted in various weather conditions showed that the noise of the highest intensity (to 60 dB) was caused by different ship engines, and it spread over considerable distances. To decrease this noise, the required AET sensitivity during the action of a compression wave on the rear wall of the protective shroud was at least 26 dB lower than the sensitivity of the AET front-working surface with which the AET was fixed to the structure surface. The application of such a method made it possible to decrease the number of the recorded AES caused by noises in seawater to only a few events per minute in one channel, and their total number for all channels was close to one event per second.

As the testing of platforms [5] showed, the AES amplitudes during crack propagation in a weld were 50…60 dB at a distance from 0.5 to 3 m from a source. At the chosen threshold level of 26 dB, the range of distances of the recorded AE events at the initial stages of fatigue crack growth in the joints of platforms at extreme weather conditions reached 2.5 m.

To provide the testing of a crack initiation and propagation in the welds of platform attachment fittings, the location of the AET should satisfy the following

conditions: For all potential AE sources, the signal damping at a distance of 20 cm for the four nearest AET should not exceed 50 dB, which corresponds to the recording range of approximately 2.5 m. This value depends on the number of welded joints through which a signal passes from a source to AET. Thus, for example, to provide the testing of an attachment fitting of a medium size, six AET are needed.

The systems of AE testing of off-shore platforms can be located both on a platform and outside it. The first one is better in a general case, because there is no need for the permanent presence of an operator. The AE data can be recorded on a hard disk and, if necessary, can be transmitted for on-shore processing. In such a case, an operative supervision over the work of a system implies periodic checking of its serviceability and replacement of disks (on average, two man-days per week).

Test results are analyzed and processed over one or two weeks. To a great extent, this period is determined by the amount of the recorded information. The major problem with AE testing is finding the location of a defect or a group of defects within the region of a platform surface chosen for the testing. The dependences of the cumulative count of AE and of the average state of seaway on time can serve as the measure of danger of defects or their groups. The results of the AE test data processing should include the following information on [5]:

1. Determination of localization of the AE sources in order to identify and group them;
2. Representation of the temporal evolution of each group of sources (cumulative count of AE depending on time);
3. Establishment of correlations with seaway for every group of the AE sources found (accounting the wave height at those moments when each AE event was recorded); and
4. Presentation of the amplitude distribution of the AE events in every group of the Hsu sources [3] (based on the signals recorded by the AET closest to this group).

From the data stored on a disk for every test period (for one or two weeks), only those of interest are preserved. Such sorting of the AE test data is performed according to the results of their analysis outside the platform, in laboratory conditions.

Except for a system of the AE testing of off-shore platforms considered above, in order to inspect the joints of a simple geometrical shape, it is possible to use a simple portable system that has four receiving AET and a calibrating generator of ultrasonic vibrations. The AET can be mounted in the region of a unit having defects and an elevated concentration of stresses, or it can be moved from one place to another where there is a danger of defects forming. Such a system can be also used to check the operation of various mechanisms placed on a platform—for instance, for checking the growth of fatigue cracks in the rings of revolving hoisting cranes [5].

6.3 Using the AE for Testing the Nuclear Reactors

The possibilities of using the AE method in diagnosing nuclear reactors were considered in many papers (see, for instance [15–17]). In particular, in [17] a problem regarding the possibility of the AE testing of the growth of defects in pressure vessels of nuclear reactors was studied both during hydrostatic tests and in operating conditions. Research was conducted in the following three directions:

1. Developing the methods of identification of crack length increment using the AES.
2. Determining relationships between the recorded AE and the crack length increment.
3. Determining a possibility to test the pressure vessels both during hydrostatic tests and in operating conditions.

The realization of this research program started from the laboratory experiments on ATM A533 B steel specimens of Class 1. However, due to the fact that a direct transfer of laboratory results to large-scale structures turned out to be very complicated, the tests were conducted on the pressure vessels with the wall thickness over 100 mm. At the third stage, the AE testing system was mounted directly on the operating reactor.

During the preparation of hydrostatic testing in the central part of a vessel of dimensions of 120 × 700 × 1500 mm, three fatigue cracks were artificially initiated: two on the internal surface and one on the external. The sizes of all three defects were different, which made it possible to obtain different rates of growth for each of them in subsequent testing.

During hydrostatic testing, water temperatures were 65 and 265 °C. Three types of AET were used for AES recording: the AET with metal waveguides twisted into specially drilled holes on the vessel surface; three AET with metal waveguides tightly pressed to the investigated surface; and low-frequency AET directly mounted on the vessel surface. These AETs were used only in hydrostatical testings.

The AE testing equipment consisted of a recording unit, where the AES that were received were processed, and their time dependences, amplitude, difference in the arrival time, and other characteristics were found. Then, this information was translated into a digital code and was stored on a magnetic tape and was simultaneously transferred to a processor, where a defect location was determined, and it was decided whether the given AES was related to the crack length increment. Based on the information gathered, the degree of defect danger was evaluated.

The dependencies of the crack depth on the number of loading cycles at 65 °C were found (Fig. 6.7) using the test results. The crack depth was estimated according to the value of the measured crack opening displacement. The internal defects propagated more quickly than the external ones, due to the action of the water.

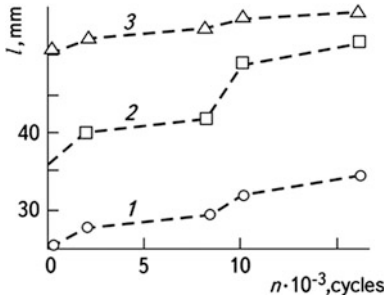

Fig. 6.7 Dependence of the crack depth l on the number of loading cycles n for temperatures 65 °C (*numbers* correspond to enumeration of cracks)

Having analyzed the AES obtained from the investigated section of the vessel, it was established that the emission from this region followed certain regularities. In all tests conducted at 65 °C, the AES had large amplitude values that corresponded to the maximum values within a loading cycle. The amplitude of over 60% of signals was higher than 9 V. Unlike the above-mentioned laboratory testing of specimens, only 8.5% of AES had similar amplitude values. Moreover, it was found that the AES were densely grouped at the maximum load value in a cycle. In laboratory research, only about 2% of the recorded signals corresponded to the maximal load in a cycle, while the majority of the AE events corresponded to the average value of the load. The information on the load value during these tests was transmitted to the AE testing system and stored. For this purpose, the cycle of loading was conventionally divided into 100 parts, and the number of each part that was stored by the system corresponded to each load value.

The dependencies of the AES count rate against time were obtained using the information on the defect location. Together with the results of laboratory tests that enabled finding the rate of the AES count, the possibility of estimating the defect growth velocity was found when no defect growth was observed. It was found that the crack growth rate, determined from AE data, was somewhat higher than that established by measuring the crack tip opening.

Except for the AES caused by the growth of artificially created defects, the AE caused by natural fatigue cracks was recorded under cyclic testing. These sources were concentrated in the area of the welds. Subsequent inspection of these welds—using the methods of non-destructive testing—confirmed the presence of cracks in them. It should be noted that signals from these cracks were recorded at distances of up to 3 m, including the most remote AET. In those tests, the AET were tightly pressed to the surface investigated. They are similarly fastened in the case of AE testing of the reactor.

A special problem of the AES research in hydrostatical tests was to estimate the possibility of detecting the fatigue cracks by means of the signals they emit. However, under periodic loading, when the applied load was 1.1 times higher than the maximum load during cyclic testing, no significant AE was recorded. The results put the efficiency of using the AE for the detection of defects in hydrostatical

testings in doubt. It should be noted that the AE activity was considerably higher when a vessel was not preliminarily cyclically loaded up to the level mentioned.

One of the major problems when designing the AE testing system for nuclear reactors is developing a method for separating the AES that are generated by a propagating crack and the signals from the sources that are safe. For this purpose, a numerical processing of signals was carried out, which permitted selecting appropriate features related to spectral composition (for instance, peculiarities of power spectrum of an individual signal, self-correlation function, or statistical moments of power spectrum). This procedure permitted decreasing the volume of information required for a description of the analyzed signal characteristics. Based on the established features of the AE pulses, the regularities were obtained, according to which the recorded signals were classified.

At first, the set of features extracted from the AE pulses did not provide satisfactory results while testing the reactor pressure vessels. Therefore, a new group of the AE signal characteristics was composed, which included the parameters of a self-regression model of the tenth order describing every individual pulse. The advantage of this group of characteristics is that it is not very sensitive to signal amplitudes. The efficiency of these characteristics was demonstrated while classifying seismic signals and while processing the AE data obtained on aluminum specimens. As regards testing reactor pressure vessels, the correctness of such a classification method was 75…80%. The authors [17] felt that despite the improvements introduced, these results still cannot be considered acceptable. The statistical analysis showed that the correct level of accuracy in classifying the defects should provide an error not exceeding 10%. Only in this case is the application of the AE testing system effective.

While testing the reactor power unit, the AE testing system included 16 AET with high-temperature waveguides, which were pressed to the surface of the reactor casing, both in the region of its bottom and near the inlet and the outlet nozzles of the cooler circulation system. The resonance frequencies of the AET were chosen in the range of 450…500 kHz. Tests were carried out at a continuous increase of temperature and pressure up to their working values (292 °C and 15.4 MPa), with subsequent holding at these values. As a result of testing, it was found that the noises were caused by the cooler flow and depended on the service conditions, i.e., values of temperature and pressure, and type of reactor, as well as on the AET type and the construction of the waveguide (Fig. 6.8). It should be noted that the values of signal amplitudes caused by fatigue crack increment presented in the figure were obtained in previous pressure vessel testing. As is clear from the same figure, at a temperature of 65 °C and a pressure of 2.6 MPa, it is almost impossible to select AES that are generated by fatigue crack growth on the background noises, even by using the AET with a resonance frequency of 500 kHz. At higher temperatures and pressure of the cooler, the conditions of AE recordings caused by a crack are much better. Thus, at a temperature of 177 °C and pressure of 2.8 MPa, and at higher values of these parameters, the AET with waveguides of a resonance frequency of 500 kHz, enables selecting the AES effectively enough on the background noises. Besides, it is clear from Fig. 6.9 that when using the high-temperature AET without

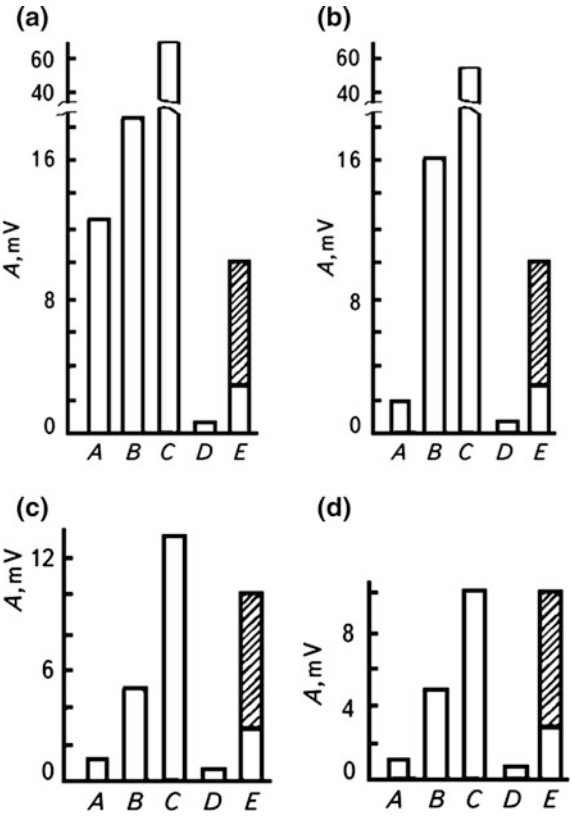

Fig. 6.8 Dependence of the cooler noise level *A* on temperature and pressure: *A*, *B* is recorded by the AET with a waveguide with a resonance frequency of 500 and 375 kHz, respectively; *C* is recorded by high-temperature AET without a waveguide; *D* is a level of electric noises; *E* is the AES level at a temperature and pressure, respectively: **a** 65 °C and 2.8 MPa; **b** 177 °C and 2.8 MPa; **c** 292 °C and 8.4 MPa; d 292 °C and 1.4 MPa

a waveguide, the AES amplitudes slightly differ from the noise level, which is why it is unreasonable to use a waveguide. Such AET efficiency can be improved by providing a waveguide and by decreasing the sensitivity to low-frequency vibrations in this way.

To check whether the AE testing system is capable of recording the AES in service conditions, a series of experiments was carried out. Compact specimens made of instrumental steel were preliminarily loaded mechanically, then mounted on the pipe and tightly fastened to the inlet pipeline. Furthermore, a heated brass bar was pressed to its surface. Due to temperature differences of the coefficients of thermal expansion, the specimen was additionally loaded and ruptured. The AES generated by the specimens that failed in this way were recorded by the AE testing system at various working temperatures, pressures, and conditions of a cooler flow.

As a result of all the tests, the following was revealed:

1. The AE testing permits revealing the increment of both artificially induced and natural fatigue cracks in thick-walled pressure vessels used in nuclear reactors.
2. The possibility of the AES detection in the presence of technological noises of the reactor is shown.

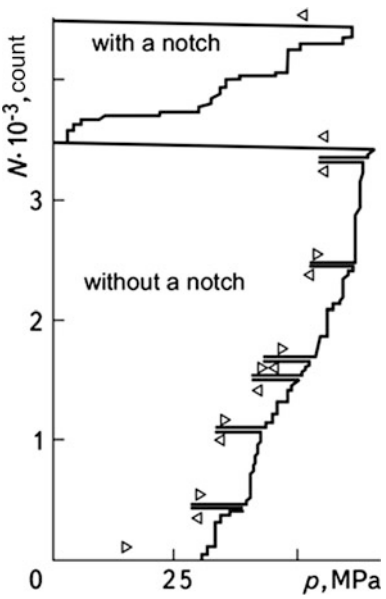

Fig. 6.9 Dependence of the cumulative count of AES N on the level of the applied stresses p under stepwise loading of a pipe without a notch and with a notch

3. The AE data can be used for the estimation of fatigue crack growth rate in thick-walled pressure vessels.
4. The efficiency of applying a high-temperature AET with waveguides in the reactor operating conditions is shown.
5. The AE system permits maintaining rather reliable and continuous testing of the state of an operating reactor for a long period of time (at least one year).
6. The AE testing system permits revealing the defects located in the sections of a reactor that are difficult to access.

6.4 Application of AE Method for Estimation of Strength of Pressure Vessels and Pipelines

Here we present some results obtained while using the AE for checking the initiation and propagation of cracks in the models of a pressure vessel and in large-scale pipelines. For the AES recording, the equipment of the Dunegan-Endevko Company, type 3000, and the multi-channel system 1032 were used [18]. This equipment permitted carrying out a spatial location, time-gating, and selecting the AES pulses according to the parameters of an external loading that made it possible to eliminate the effects of external noise sources and to select information on fracture for subsequent processing and reproduction in a printed form or in a display.

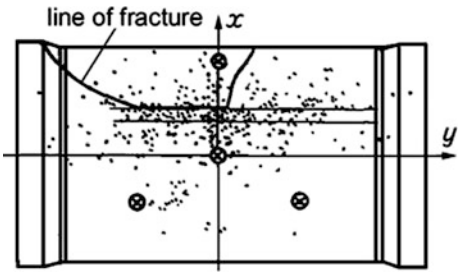

Fig. 6.10 Determination of the coordinates of the AE sources in the region of a weld failure by four AET for the whole observation period

In Fig. 6.10, the results of the AE recording under stepwise loading of the pipe with a 210 mm diameter and 40 mm thick wall made of 12X1MF steel are presented. An external notch located in the axial direction was made on this pipe. Its depth was 0.45 of the wall thickness, and the length was 250 mm. While loading the notched pipe (Fig. 6.10), the AE from the notch region was recorded at a slight internal pressure that confirms the development of this defect. This was also proved by the results of the location of AES due to the fatigue crack increment. The location of AE sources permits estimating the crack sizes and establishing the location of an initiated crack.

Furthermore, a piece of a pipeline of 850 mm in diameter and a 48 mm thick wall made of 22K steel with anticorrosion X18N10T steel coating welded on the internal pipeline was tested. The pipeline contained longitudinal welded joints that provided a considerable heterogeneity of the stress-strain state. The defects that unavoidably arise during welding also reduced the serviceability of the pipeline. The results of the AE sources' location in the area of each longitudinal joint during the loading, up to the moment of failure of the section of the pipeline that was examined, are presented in Fig. 6.11. When the pressure increases, the AE sources that form groups in the area of the welded joints indicate the areas of the location of the defects that develop during testing. At a pressure of 40 MPa, the pipeline fails. It was established that in the area of crack growth, the fracture was caused by the

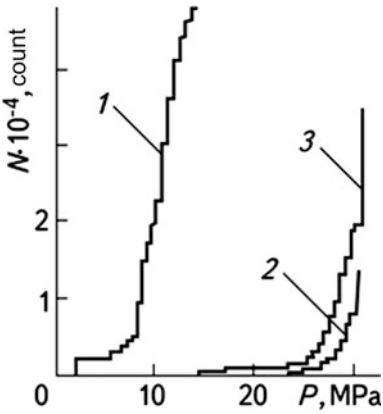

Fig. 6.11 Dependence of the cumulative count of the AES N on the level of the applied stresses P during hydraulic testing of a section of 22K steel pipeline with cracks (*1*) and welding defects in the area of longitudinal welds Nos.1 (*2*) and.2 (*3*)

Table 6.3 Data on a crack length increment in a pressure vessel

Region of longitudinal welded joint	Notch depth, mm	Notch length, mm	Final crack depth, mm	Number of loading cycles for a visual revealing
Base metal	10	100	13.0	5800
	14	140	24.3	3000
Welding metal	10	100	13.0	6300
	14	140	18.8	3390
Heat-affected zone	10	100	13.0	6000
	14	140	20.8	3200

presence of faulty fusion welding in the joint area of the base metal, surfacing, and the welded metal of a weld. Herein, the AES recording made it possible to find a defect that develops long before a complete failure of the examined pipeline section.

Repeated static testing by internal pressure of real sections of straight pipelines made of 22 k steel with anti-corrosion coating of X18N10T steel of a diameter of 850 mm and wall thickness of 48 mm that contained circular and longitudinal welded joints were carried out as well. In the base metal and in the coating, as well as in the heat-affected zone of longitudinal welds, there were surface notches with a depth of 0.25…0.35 of the wall thickness. Apart from these notches, welding defects of sizes that exceed the admissible ones were left without healing in a welded material. During testing, the loading parameters were recorded, and, using the AE testing system, the AE sources were localized and the AES parameters were recorded. The test results of one of the pipeline sections are presented in Table 6.3 (maximal nominal hoop stresses were 0.8 σ_{02}, while the number of loading cycles of all modes was 7500).

The analysis of recorded AES alongside the visual observation permits proving that the crack initiation conditions are different in different regions of the welded joints; this is explained by the difference of material properties and the presence of typical residual stresses. Therefore, the cracks that started from the notches of identical size but were located in different regions of the welded joints, began to propagate after a different number of loading cycles. The moment of their growth start was revealed much earlier by means of AE than by visual control.

A high concentration of the AE sources in certain areas of a structure and the fact that AES was recorded in the narrow range of the applied load that corresponded to the threshold stress intensity factor values, confirmed the beginning of the crack propagation. It should be noted that this range for the cracks located in different regions of the welded joints was also different, thus proving that the dependence of fatigue crack growth kinetics on heterogeneity of the stress state is related to the material properties in the region of the welded joints. As a result, the depth of fatigue crack growth under the same modes of loading at identical initial sizes of notches was different.

The AES caused by cracks initiated at the notches and at the natural welded defects were recorded separately during the hydraulic testing of pipelines. The results of these tests are presented in Fig. 6.11. It was found that the AE activity caused by the defects that develop from the notches of a depth equal to 0.35 of the wall thickness was higher than by the welded defects. Shallow defects (the notch depth equal to 0.25 of the wall thickness) produced the AE, which was practically the same as the welding defects. Metallographic analysis confirmed the availability of a slight crack growth at small notches and near the welded defects.

Thus, the AE method permits defining the location of the AE sources and their activity, which enables one to conduct the analysis of a structure's imperfectness. The inspection of the AE sources that were found can be further conducted using traditional methods of non-destructive testing, which take into consideration the available standards and provide information on the degree of danger of the defects.

The information obtained using the AE method during hydraulic testing [18] can be used for the operation inspection of pressure vessels and pipelines. In this case, it is enough to check only the areas of the AE activity revealed during hydraulic testing. Based on these observations, it is also possible to establish the specific features of the development of defects, to solve the problem of technical diagnostics, and to predict the lifespan of the equipment.

6.5 AE Inspection of Welded Joints

Most unique structures contain welded joints that should be highly reliable when being used, and special diagnosing systems and complexes have been developed for this purpose. As is known, means of non-destructive testing and diagnostics, which use the AE method, permit testing the required volume zones of a structure or its individual elements regardless of geometrical sizes and the type of material. The defects in the welded joints (gas pores, tungsten inclusions, oxide films, cracks, faulty fusion, etc.) non-uniformly distribute the loads over the volume of the tested object which, in turn, causes some differences in the AE generation due to the availability of the areas with and without defects. Therefore, to effectively use the advantages of the AE method as one of the promising methods of nondestructive testing, one needs to have the preliminary comparative characteristics of the AE activity of structural materials under loading, when the processes of defects initiation and propagation in them are observed, i.e., fracture processes. This enables us to select the necessary conditions of recording the AE signals by a measuring device, to compare the optimum values of their information parameters, such as amplitude, cumulative count of the AE signals, number of events, spectral characteristics, etc., as well as to maximally approach the solution of the problem of signal identification. Such investigations of structural materials and their welded joints are carried out in laboratory conditions and form the basis for the development of new methods of diagnostics and non-destructive testing of products and constructions.

The quality of a welded joint can be inspected using the AE method at different stages. The first stage includes the period of welding from the very start until the end. The second stage includes the period of the weld cooling until it reaches its equilibrium state. The third stage includes the period following the establishment of the equilibrium stage.

The AE testing of extended welds can be carried out simultaneously at the first two stages. Their common feature is that the AES originate under the action of internal local stresses that develop in a near-joint area without additional external loadings (Fig. 6.12). Internal stresses are caused by the material structure heterogeneity, as well as by non-uniformity and non-stationarity of thermal conditions of the process of welding. At the second stage of inspection, a common or local external action on a weld is necessary for the AES generation.

A successful application of the AE for weld testing is related with a possibility to select signals generated by defects from the general amount of signals that are generated against the background noises. A frequency band, in which the AES are selected, is chosen, taking into consideration the spectrum of noises and acoustic waves damping in the material. Usually, this frequency band is set within the interval of 50 kHz…2 MHz.

The AE testing of pipe welds is performed, as a rule, during the cooling of joints, expanding, or hydraulic testing of pipes [19]. During hydraulic tests, the recorded AES were caused mainly by the noise due to the water flow and its friction with the pipe wall, and due to slight leakages that were not recorded by a manometer. However, at hydraulic testing, the defects do not emit AES. As the analysis showed, this is explained by a volume expansion immediately before a hydraulic testing of a pipe, when much stronger forces compared with hydraulic testing are applied to it, and thus the KE is observed.

During expanding the pipe is deformed successively in the sections of length of about 1 m. The degree of deformation attains 0.5…0.7%. In this case, as research

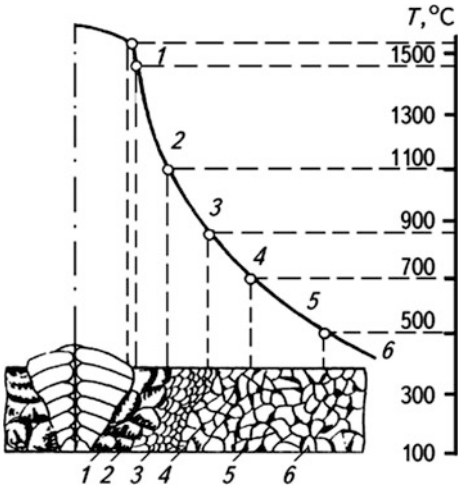

Fig. 6.12 Schematic of temperature limits distribution in the near-weld zones: *1* is the melt area, *2* is the overheat area, *3* is the re-growth area, *4* is the incomplete recrystallization area, *5* is the recrystallization area, *6* is the aging area [9]

has showed, it is very difficult to detect cracks using the AE method, due to the high level of noises caused by plastic deformation of material and by friction of expander elements with the internal pipe surface. During welding, it is difficult to reveal the cracks due to the noise caused by slag film cracking.

More optimistic results were obtained in the AE research at cooling the welds. During their cooling, the AES are emitted with defects for a long time and are characterized by high amplitude and intensity. Specimens with high-quality welds practically do not emit the pulses, and only single rare bursts of the amplitude and intensity are observed (Fig. 6.13) [20]. A slag layer is removed from a weld immediately after its welding. According to the investigation results a good correlation was founded between the longitudinal and transversal cracks and the AES in welds; however, in the case of volume defects (such as pores), the AE was not practically observed.

The welded structures are subdivided into 4 groups according to AES radiation intensity: 0—AES is practically not observed; 1—insignificant intensity of AES radiation (up to 104 pulses); 2—AE of medium intensity (up to 4×10^4 pulses) with the considerable AES amplitudes; and 3—continuous AES of high intensity (up to 12×10^4 pulses).

The initial basic data on the AE character is required for each particular case of the welded joints that would take into account the structure of materials, technology of their welding, and so on. Such data are definitely obtained during laboratory testing. We will briefly discuss some of this data.

6.5.1 *Verification of Selection of Materials, the Type of Specimens, and an Investigation Method [21]*

An improvement of reliability of the welded structures takes place with a simultaneous decrease of steel intensity and is a basic direction of the development of

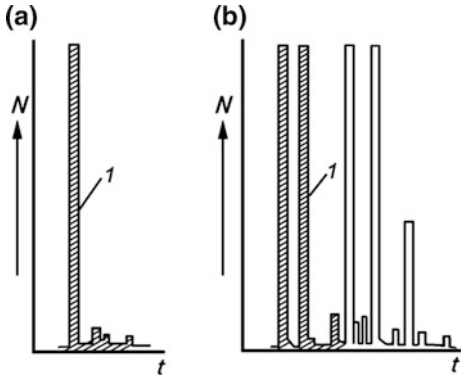

Fig. 6.13 Change in the cumulative count of the AES N with time t in the case of high-quality (**a**) and low-quality (**b**) welding. *1* are hindrances from a welding arc

science dealing with welding. The tolerance of this or another technological defect of a welded joint can be established today regardless of the structural element location, its stress state, number of cycles of loading alternation, residual stress, etc. The absence of a profoundly considered differentiation of the damages of the materials of the welded joints according to corresponding standards often causes the premature fractures of the welded joints due to defects, while in other cases the defects are quite groundlessly withdrawn without proper consideration. It is well known that the defects being cut off from a component with the following welding does not increase but rather decreases the load-carrying capability of the component. The problem becomes more urgent taking into account the fact that about one-third of all premature fatigue fractures of metal structures, machines, and buildings, reservoirs, and pressure vessels, special technological equipment, etc., are today conditioned by the defects of welded joints [22].

In the world of engineering practice, the production of vitally important welded structures, such as ships, multi-storied buildings, power equipment, aviation and space objects, etc., is accompanied by the allocation of considerable financing for the implementation of facilities and methods of non-destructive testing and diagnostics. A fraction of these finances in some cases reaches 20–25% of the total cost of structures, while labor intensiveness becomes almost the same as for the welding processes [23]. The analysis of the welded structures' failure shows that in most cases it takes place in the near-weld area rather than along the weld. This is explained by the fact that the weld is more durable than the base metal. Thus, the thickness of a strengthening roll under two-sided welding is 1.8…2.2 times higher than the wall thickness. Besides, the weld metal is micro-alloyed with a cast structure. The structure of the near-weld area for arc, plasma, and electro-slag processes is heterogeneous and has considerable residual stresses. Structural transformations in a metal, and considerable plastic strains, appear due to abrupt changes of temperature in this area. The defect at the base metal ends arising due to temperature effect and deformations increase their volume and become dangerous [24]. Herein, a very negative effect of hydrogen should be noted, which in the atomic state is released into micro-cavities during the welding process, and later on having transformed into molecular hydrogen, creates high pressures in them and, as a result, we observe high stresses in the metal. It is the hydrogen mechanism that forms the basis of the phenomenon of the so-called "cold cracks initiation" and propagation in the weld metal and in the heat-affected zone [25, 26]. Thus, taking the above into account, the specimens of structural materials made of the base metal (BM), weld metal (WM), and fusion zone (FZ), became the object of the AE studies.

One of the peculiarities of inspecting the quality of the welded joints using the AE method is that pre-conditions for its realization are available at different stages of the technological process: during welding; during the formation of a joint and after welding; and at transition of the welded joint into the equilibrium state or after termination of this process [9]. All these stages are clearly expressed in the methods of welding, which are related to melting. At the first two stages, the AE is generated under the action of internal stresses, while at the third stage there is an additional local action of an external loading. Exactly then (at temperatures lower than 100 °C), deformation

cracks, corrosive cracks, and deformation-corrosive cracks are formed [26]. The first type includes cracks that appear in welds after their cooling and in the process of aging after welding, as well as cracks that appear in a metal during tensile deformation, compression, impact, and other types of mechanical action. The second group includes cracks whose initiation is predetermined by the action of only one corrosive environment without applying an external loading, and the third type of cracks appears in a metal under a simultaneous action of an external loading and a corrosive environment. During exploitation, the cracks that appear due to various strengths of some elements of a structure and phases (for instance, eutectic inter-layers, non-metallic inclusions, pores, etc.), and due to the action of external loading forces appearing in the process of product exploitation, are effectively revealed by the AE method. Thus, in this study we investigate the methods that use the AES testing of the fractured welded joints caused by a quasi-static loading, i.e., the methods for estimation of the static crack growth resistance of a welded joint.

The trends in the development of welding technologies are characterized by the transition to low-alloy steels with a simultaneous reduction of the amount of metal in structures and by an increase of reliable service life. This is confirmed by the fact that today about 20 grades of low-alloy steels are used exclusively for building structures, and, taking into account the quality categories, their number has increased more than threefold [22].

At the same time, in many branches of industry, non-ferrous metals are widely used as structural materials in manufacturing vitally important units and even whole structures. Aluminum alloys are of special interest. Therefore, as representatives of the above-mentioned different grades of structural materials, the steels 10XSND, 09G2S, Steel 3sp, as well as 1201-T aluminum alloy were chosen. Specimens made of these materials were constructed with the account of three-point bending loading or eccentric tension [27], while cylindrical specimens used for the evaluation of mechanical characteristics of 1201-T alloy met the requirements of [28].

According to the test method, the AE signals were recorded under the loading of specimens in a real-time scale. The relationship between the AE (amplitude, cumulative count N of the signals, spectral characteristics) and fracture parameters (stress intensity factor, deformation, crack length increment), and the validity of the KE were established using the test results. Thus, the energy of the AE signals that accompany the processes of the fracture of welded joints was estimated in order to use the obtained results in non-destructive testing of the real products or structures.

6.5.2 *Results of the AE Research of the Welded Joints and Their Interpretation*

Investigation of the AE indices of fracture of low-alloy steels and their welded joints. Prism-like specimens of 6 × 15 × 170 mm were prepared for testing the 10XSND, 09G2S steels, Steel 3sp., their welded joints, and FZ. The chemical composition is presented in Table 6.4. In these specimens, after mechanical

Table 6.4 The chemical composition

					Elements	Content	%						
Alloy grade	C	Mn	Mg	Si	P	S	Cr	Zn	Ni	Al	Cu	As	Fe
Steel 3sp	0.14…0.2	0.40…0.65	–	0.12…0.30	≤0.045	≤0.055	≤0.3	–	≤0.3	0.013	≤0.3	≤0.08	*
09G2S	≤0.12	1.3…1.7	–	0.5…0.8	≤0,04	≤0.04	≤0.3	–	≤0.3	–	≤0.3	–	*
10XSND	≤0.2	0.5…0.8	–	0.8…1.1	≤0,04	≤0.04	0.6…0.9	–	0.5… 0.8	–	0.4…0.65	–	*
1201-T	–	0.3	0.02	0.03	–	–	–	0.03	0.03	*	6.5	–	0.14

*—Other

treatment by a polishing stress, notches were cut out and then fatigue cracks were induced. Specimens were made in such a way that in the working area, i.e., in the net-section, there was a failure in BM, WM, and FZ. The SVR-5 [29] loading machine that was used to apply a load differed from serial loading devices by a low level of generation of background noises. This permitted selecting the AES at high amplification levels and at low threshold levels in the AE channel [30].

The scheme of testing the specimens was as follows [31]: The loading forces were transmitted from the SVR-5 equipment through an indenter to the investigated specimen, on which the AET was mounted to its lateral surface. The force of pressing the AET with a clamp to the lateral surface of the specimen through a contact layer [3, 32] was 15…20 N. During loading, the diagram "load P − crack opening v" was recorded by an X-Y recorder, while the amplitude A and cumulative count N of the AE signals were simultaneously recorded by a fast-acting recorder H-338/4 in real time. After pre-amplification and processing the AE signals by the AVN-3 device, these parameters were printed on paper.

Before every experiment, a measuring channel was calibrated by the Hsu source. The MBS-9 microscope supplied with a set of the SVR-5 equipment was used to inspect the changes at the lateral surface of a specimen in the crack propagation region. Taking into account the high plasticity of steels (Table 6.5) at room temperatures [32] and service characteristics of a loading machine, we have chosen the following modes of the AE selection and processing: Mode I: amplification factor of a measuring path is equal to 74 dB, threshold level of the AE signals is equal to 0.4 V, working frequency band Δf is equal to 0.12…0.5 MHz with the transmission coefficient of filters of low and high frequencies equal to one. The AET possesses, accordingly, the best working characteristics in the frequency band from 0.2 to 0.5 MHz. The results of testing 10XSND steel specimens, their welded joints, and FZ material obtained in such measurement conditions, are presented in paper [33]. Therefore, we will briefly discuss some of them.

The AE signals were recorded both for the linear area of diagram "P-v and for the non-linear area up to the moment of the final macro-fracture stage. Their amplitudes at the analog output of an AVN-3 device were in the range of dozens of mV to several volts. The AE signals were most actively generated during the testing of the specimens cut out of the welded joint metal, and then with a decrease of amplitude, the number of events, and the cumulative count, there come

Table 6.5 Mechanical characteristics of alloys

Alloy grade	σ_{02}, MPa	σ_b, MPa	δ, %	ψ, %	F_b, %[a]	K_C, MPa$\sqrt{m}$
Steel 3sp	280	430	26	55	92	56.8
09G2S	330	500	28	58	77	69.2
10XSND	400	540	24	50	97	58.3
1201-T	350	440	4.75	7.54	–	44.3 38.04[b]

[a]F_b, is the fraction of a ductile component in a ruptured specimen at t = 20 °C [32]
[b]Is the K_{1C} value

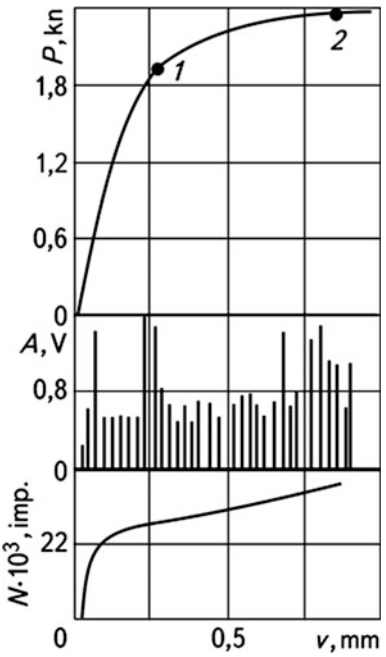

Fig. 6.14 Fracture diagram "*P-v*" (three-point bending) for the metal of FZ of a welded joint of 10XSND steel and corresponding distribution of the AES amplitudes *A* and cumulative count *N*

the specimens cut out of BM and WM. Thus, for 10XSND steel and its welded joints, it is shown that the value of amplitudes and intensity of the AE generation at a sub-critical crack propagation in specimens from various welded joint areas are sufficient to be recorded during testing of large-scale structures or the products under static loading (expanding). Then, the industrially produced equipment of the AVN-3, AF-15 types and others can be used. As the experimental data (Fig. 6.14; Table 6.6) argue, there is a margin in the amplification and threshold levels; thus it is possible to reduce the amplification and to increase the threshold level. The AE testing and diagnostics efficiency can be substantially improved using a resonance or narrow-band AET, as well as by using certain methodological approaches to the selection of the AE signals under the effect of sensible background noises [34] in real conditions of diagnostics.

Welded joints of 09G2S steel and Steel 3sp were investigated using a similar scheme. The AES registration regime differed from the previous one by the amplification factor, which was 84 dB, and by the threshold level, which was 0.2 V (Regime II). The other measurement parameters, geometry of the AET location on the specimens, and calibration of measurement path sensitivity were the same. The shading of the area of the crack length increment was done by heating the specimens in an autoclave to a temperature of 300…350 °C and by holding them at this temperature for 600 s with the following impact rupture of the specimens after cooling.

Table 6.6 Results of the AE research

Alloy grade	Area of specimen cutting out	K_I, MPa$\sqrt{m}$	Number of events	Sum of amplitudes A, V	Cumulative count N, 10^3, counts	Maximum amplitude at the AET output A_{max}, mV	Area of crack increment, S, mm^2	Measurement mode
Steel3sp	BM	23.4	23	2.68	5.2	0.027	–	II
	WM[a]	28.3	49	3.4	2.2	0.035	–	
	FZ	34.0	240	15.44	14.5	0.25	–	
09G2S	BM	29.4	96	7.68	9.5	0.05	–	II
	WM	34.4	122	7.24	8.3	0.025	–	
	FZ	32.1	121	8.84	13.0	0.025	–	
10XSND	BM	16.5[b]	246	18.36	19.02	0.104	–	I
	WM	33.15	126	7.72	1.78	0.067	–	
	FZ[1]	32.8	258	65.36	24.2	0.335	–	
	FZ[2]	40.46	376	22.82	38.15	0.335	3.2	
1201-T	BM	440[c]	324	0.14	0.82	0.015	–	III
	WM	42.56	46	0.33	16.8	0.89	173.25	

[1]Point 1 in Fig. 6.14; [2]point 2 in Fig. 6.14

[a]The faulty fusion cavities of the area of up to 4 mm^2 are detected on fracture surfaces

[b]Linear area of the fracture diagram

[c]σ_b value for cylindrical specimen tension

As seen in Fig. 6.14, to develop the criteria approaches in laboratory conditions, it is worth recording the AE signals in the loading ranges of specimens to a certain value in the non-linear area of the fracture diagram (points 1, 2 in Fig. 6.14). This is confirmed by the fact that in real loading conditions under large plastic deformations, the defects in ductile steel structures are easily revealed visually, and in this case the macro-crack opening attains considerable value.

Specimens of 09G2S steel and Steel 3sp were loaded until a plasticity area on the diagram *P*-*v* appeared; then they were unloaded, and the value of the fatigue macro-crack length increment was calculated, as stated above (Table 6.6). The test results confirm the following: The energy level of signals that accompany the processes of initiation and propagation of micro- and macro-cracks for three grades of steels is the lowest for Steel 3sp. After that, according to an increase of this index and AE activity, come steels 09G2S and 10XSND steels. Concerning the welded joint areas, all grades of steels prove the above regularity of ordering for 10XSND steel: FZ, BM and WM. Besides, for materials of all the welded joint zones, the KE is satisfied [33, 35].

Estimation of peculiarities of generation of the AE signals due to fracture processes in welded joints of 1201-T aluminum alloy. Investigations were carried out in two stages: In the first stage, the BM mechanical characteristics were calculated [28], and simultaneously the AE that accompanies the processes of plastic deformation, macro-crack initiation and propagation was recorded. For this purpose, cylindrical specimens with a diameter of 4 mm were prepared. They had a thick part in front of a threaded part on both sides, where flats were made for mounting the AET [36].

Before each test, specimens were subjected to molding in a special conductor according to the method presented in [37] for removing the non-informing AES emitted from the grips area during loading. Loading forces exceeded the admissible level by 50…80%. After that, the experiments were conducted. A tensile-testing machine of the FPZ-100/1 model with the speed of traverse movement of 0.02… 0.84 mm/min was used as a force-inducing device. The AE chain of selecting, processing and recording the AES was built, based on the AE MISTRAS—2001 system produced by PAC (USA), to which analog signals from the strain gauge force dynamometer from the machine FPZ-100/1 were transmitted, together with the displacement gauge for measuring the value of the specimen elongation or crack faces opening (depending on the type of the specimens tested). Simultaneously, signals from the AET with a working frequency band with linear amplitude-frequency characteristics within the range of 0.1…1.2 MHz were transmitted to the AE chain through a preamplifier. The preamplifier amplified the AES by 40 dB in the path band of 0.02…1.2 MHz, while the threshold level of the AES was 45 dB. The following AES parameters were obtained in this mode of selection and processing (Mode III): time rising to the maximum of the forward front of a signal τ_1, duration of the AE signal above the threshold level τ_2, amplitude, number of pulses *N*, energy *G*. Furthermore, the measuring system made it possible to receive spectral characteristics of the AE signals from their waveforms.

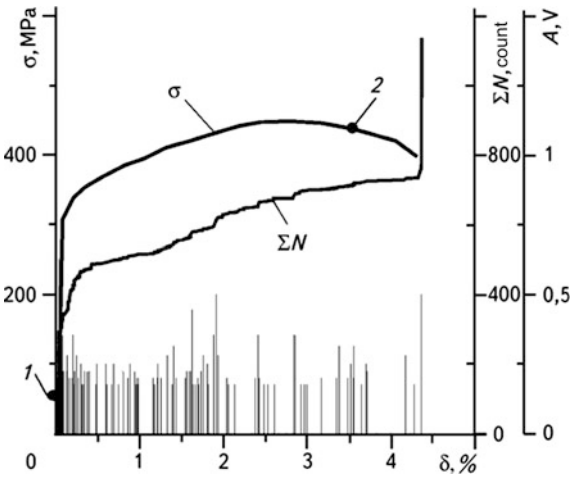

Fig. 6.15 Stress-strain diagram σ-δ of a smooth cylindrical 1201-T alloy specimen and the dependence of a cumulative count N and signal amplitudes A on the strain δ of a specimen

In the second stage, the AE characteristics of fracture processes in materials of 1201-T alloy weld were investigated on 79 × 79 × 7 mm compact specimens, which were manufactured according to standards and typical ratios of geometrical sizes, given in [27]. Welded joints were made by means of electron-beam welding. Figure 6.15 shows a typical diagram of tension and distribution of AES arising in a cylindrical specimen, and Fig. 6.16 presents spectral characteristics for points 1 and 2 of this diagram. From the last figure, it is seen that the AES amplitudes that arise during the process of macro-crack initiation and accompany the appearance of cracks in various inclusions in a material [36] at initial stages of a stress-strain diagram, are of slight magnitude (measured in mV). The main activity of the AES is concentrated in the range of the relative elongation δ change of a specimen within the limits of 0.1…0.4%.

The generation of the AE signals of the BM of 1201-T alloy is lower in comparison with the AE amplitudes of steels during macro-crack growth. With the growth of σ, the spectra of signals (Fig. 6.16) tend to narrow, and dominant frequencies of signals are shifted towards the low frequency values, which concurs with the results of [38]. Figure 6.17 shows the fracture diagram P-v of a WM of a welded joint of 1201-T alloy and the corresponding distribution of AES during sub-critical crack propagation, where AE signals are of a specific character. A slight amount of the AES of large amplitudes is observed, which confirms a jump-like propagation of the macro-crack and the absence of the AES of small amplitudes. This means that the mechanism of sub-critical macro-crack growth is quite brittle, and its diagnostics requires an accurate interpretation of the AES taking into account the initiation and the development of micro- and macro-cracks. The characteristic spectra of the AES in various areas of a fracture diagram confirm the above-described tendency of the change in a spectrum width and in dominant frequencies of AE.

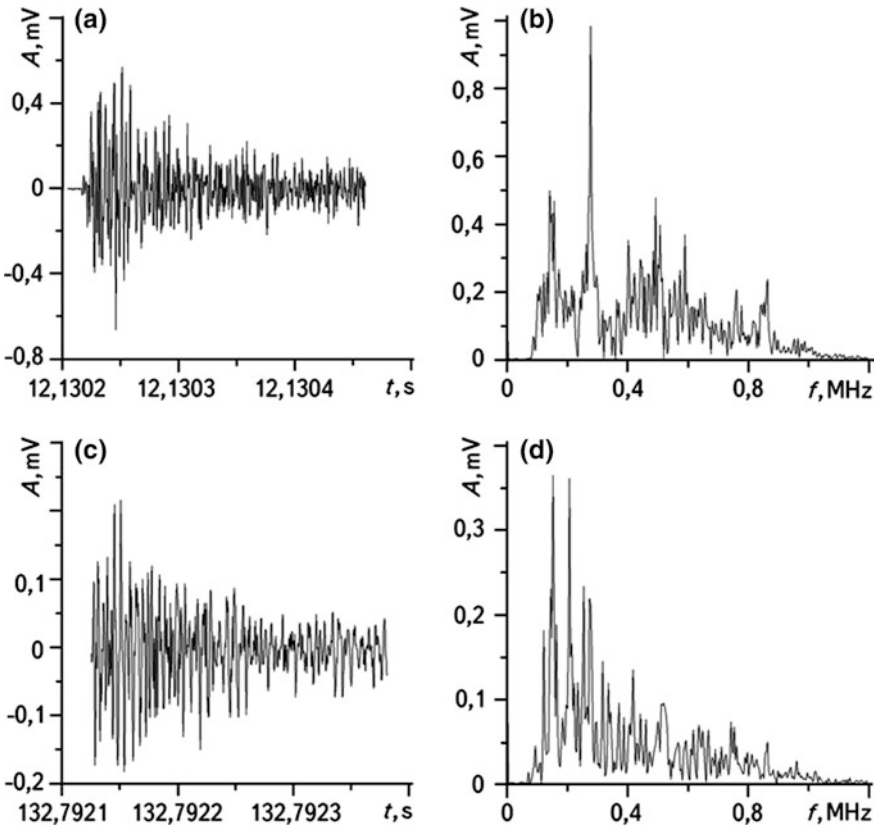

Fig. 6.16 The AES waveforms and their spectral characteristics at point *1* (**a** and **b**, respectively) and at point *2* (**c**, **d**) of stress-strain diagram (Fig. 6.15) of cylindrical 1201-T alloy specimens with the following indices of measuring modes: sampling frequency of the AE signal—4 MHz, sampling number—1024, threshold level—0.178 mV; **a** $\tau_1 = 21$ μs, $\tau_2 = 152$ μs, $N = 15$, $G = 2$ μJ; **c** $\tau_1 = 1$ μs, $\tau_2 = 1$ μs, $N = 1$, $G \approx 0$

Thus, experimental AES investigation of fatigue crack growth resistance of welded joints of low-alloyed steels 10XSND, 09G2S steel and Steel 3sp, as well as of 1201-T aluminum alloy, being the most widespread materials, showed that quantitative indices of the AE events, cumulative count, and the amplitude-frequency characteristics of the AES are specific for every type of material and for particular areas of the welded joints, which enables making a complex evaluation of the mechanisms of generation of the AE signals at the stages of plastic deformation development and the beginning of sub-critical macro-crack propagation. Using the AES spectral analysis, it is necessary to preliminarily achieve the best reproduction of a waveform of every AE event with the account of reflection, damping, and resonance peculiarities of the tested material of a product or of a structural element.

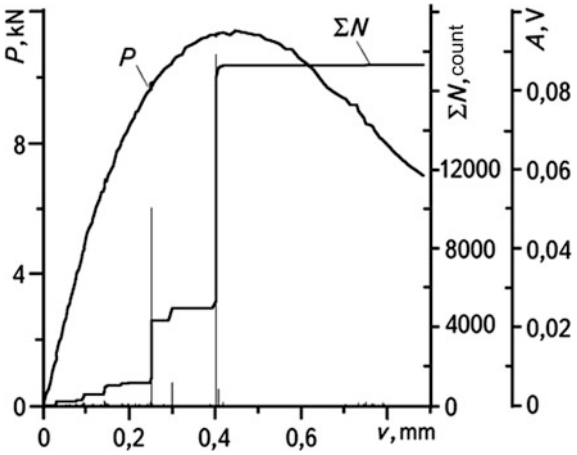

Fig. 6.17 Dependence *P*-*v* for the eccentric tension of compact specimens of a welded joint WM made of 1201-T aluminum alloy and the change in indices of the cumulative count *N* and amplitudes *A* of the AES that accompany the fracture processes

6.6 Selective On-Line AE Hydraulic Testing of an Oil Storage Reservoir

The purpose of the AE testing of a reservoir with a capacity of 75,000 m^3 is to reveal, on-line, the initiation and propagation of the crack-like defects and to evaluate the degree of their danger during hydraulic testing. To record the AES, a two-channel AE system "AKEM" (a programmable-technological complex) was used that permitted estimating the IO state by certain AE criteria. The system is mobile and provides on-line processing of the recorded information and its corresponding representation after termination of AE tests. Its characteristics are:

- Working band of frequencies—100…2000 kHz;
- Non-uniformity of amplitude-frequency characteristics of the amplification path
  - within the frequency band—not larger than ±3 dB;
- Damping of the AE signal outside the working range during the change of threshold
  - frequencies—not less than 30 dB per octave;
- Input resistance of preamplifier—1 MΩ;
- Input sensitivity—not less than 10 μV;
- Dynamic range of amplification—40…72 dB;
- Cut-off band of high-frequency filter—9 kHz;
- Effective voltage of the noise in an amplifying path—not higher than 8 μV;
- Amplification factor of an amplifying path—not less than 60 dB; and
- Amplitude dynamic range of an amplifying path—not less than 50 dB.

A set of devices and equipment that are used for AE testing included the AET with the devices for their installation on IO and materials for providing the acoustic

coupling, imitators of the AE signals, and a corresponding software. A chart of a programmable-technological complex "AKEM" used for nondestructive testing of a reservoir is presented in Fig. 6.18.

For research purposes, the AET with the working frequency band of 100… 1200 kHz were used. They were mounted directly on IO by magnetic holders. The amplitude-frequency characteristics of the AET are shown in Fig. 6.19.

Chemical non-aggressive "Ramzay" oil was used as an acoustic contact environment for the AET, which provided an effective acoustic coupling of AET with an IO. In the place where the AET was mounted, the material surface was subjected to mechanical treatment.

6.6.1 *Some Methodological Features of AE Testing of a Reservoir*

Taking into account the preliminary inspections of a reservoir by means of other non-destructive test methods, a method for on-line exclusive AE testing of the most dangerous parts of an IO liable to fracture was developed. Calculations and the available experience of the AE testing on other objects showed that in this case, these dangerous places are near-bottom joints of a shell and the location of welding of flanges, stripping hatches, etc., which is why the AET were mounted on the IO as close as possible to the indicated places for inspection.

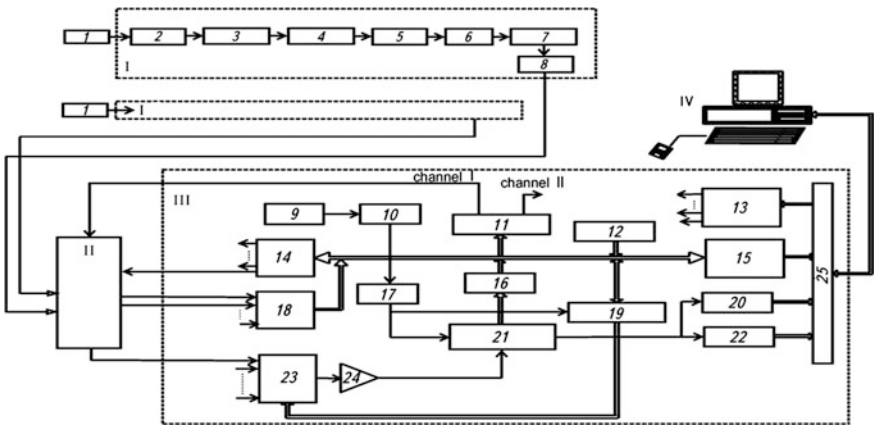

Fig. 6.18 A chart of a programmable-technological AE-complex "AKEM": *I* is AES amplification path; *II* is a former; *III* is a port of data in-out; *IV* is a computer; *1* is an AET; *2* is an emitter follower, *3* is a preamplifier; *4* is a high-frequency filter; *5* is an amplifier; *6* is a detector; *7* is a low-frequency filter; *8* is an output amplifier; *9* is a generator of 10 MHz; *10* are counters; *11* is a DAC; *12* is a status controller; *13* is an address decoder; *14* is a 16-bit output; *15* is a data buffer; *16, 17, 19, 20, 22, 23* are units of logical control; *18* is a 16-bit input; *21* is an ADC; *24* is an amplifier; and *25* is a personal computer bus

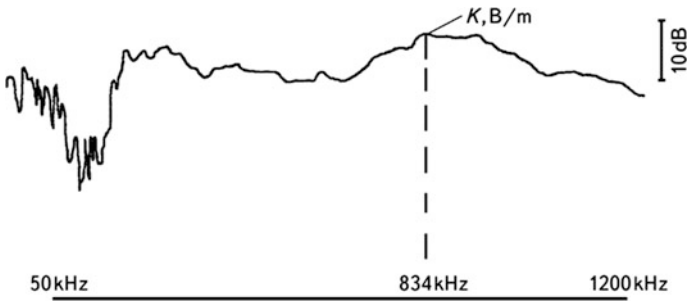

Fig. 6.19 Amplitude-frequency characteristics of the AET used in the AE testing

Taking into account the overall size of a reservoir according to State Standard 4227-2003, it was decided to carry out multi-channel AE testing. During the testing of four channels of the AE system, "AKEM" was used. Before beginning the measurements, according to the requirements of a Standard of the European working group and the requirements of the National Standards of Ukraine, calibration of the sensitivity of the AE path of all channels was performed using the Hsu source. Calibrated in such a way, the channels of AE device were adjusted to the same sensitivity as the elastic vibrations received from the sites of initiation and propagation of crack-like defects (Fig. 6.20).

Proceeding from the above, during hydraulic tests with a simultaneous filling of the external and internal casings of a reservoir, the AET were located on the opposite sides of a structure at the +1.7 m mark on the external casing, as is shown in Fig. 6.21.

In hydraulic testing of the reservoir internal casings, the AET were placed on the internal case of the reservoir according to the chart in Fig. 6.22. In all types of testing, the AE device was located outside the reservoir protective area, in accordance with the accident prevention regularities.

The AES were recorded by four channels during the growth of reservoir loading, and the load was kept at specific levels for an IO for 15 min with technological

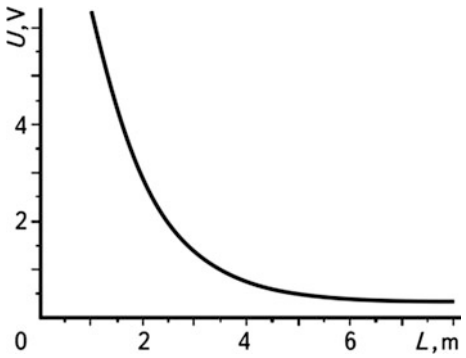

Fig. 6.20 Dependence of the change in amplitudes of AE elastic waves on the distance of AE generation by a Hsu source

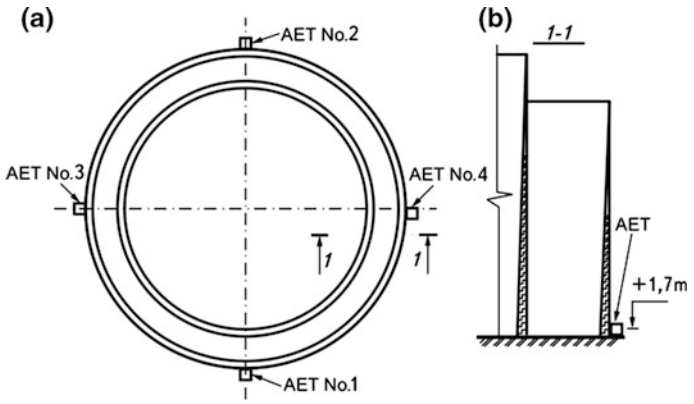

Fig. 6.21 A chart of the AET location during hydraulic testing of the reservoir external casing

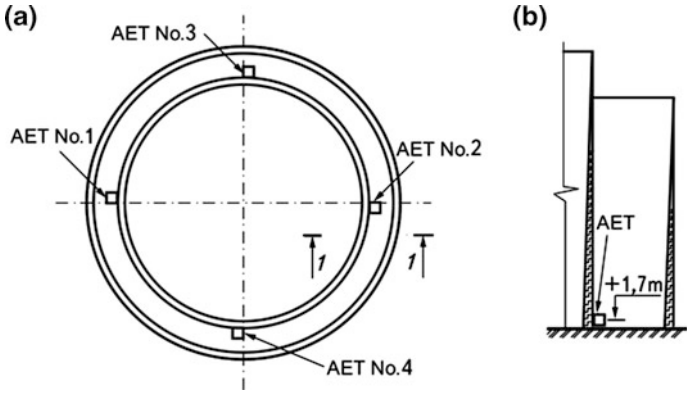

Fig. 6.22 The AET location during hydraulic testing of the reservoir internal casing

interruptions for 4 min. The AE information recording was realized as a continuous monitoring of an object. When the filling of a reservoir with water stopped, the time of the AES recording was 5…6 h.

The external reservoir was filled according to the schedule of testing (Fig. 6.23a), and the internal reservoir—according to the plot in Fig. 6.23b.

The AE criteria taken into consideration during the reservoir testing were as follows: a rapid growth of cumulative count of pulses, their amplitudes, total energy, or the energy that confirms the accelerated growth of defects that caused a fracture. If the parameters of one of the criteria reached a critical magnitude, then a stop of the technological process of reservoir filling was provided in order to investigate the nature of the AE source and estimate the possible danger of further testing.

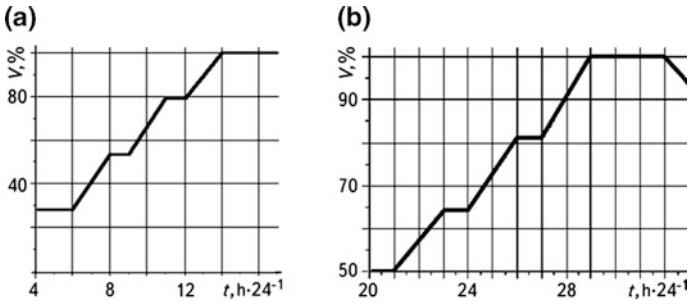

Fig. 6.23 Plot of hydraulic testing of external (**a**) and internal (**b**) reservoirs

6.6.2 *Criteria for Classifying AE Sources*

The coefficient K_p for determining the AE signals caused by cracks characterizes the degree of the energy density change in the recorded AE signal and is used for revealing the crack-induced signals. The following formula is used for evaluation:

$$K_{pj} = lg\left(E_{cj}/\tau_j^2\right) + B + C, \tag{6.20}$$

where: E_{cj} is the energy caused by the j-th recorded AE signal; τ_j is the duration of the recorded AE signal; B is the correction factor for the device sensitivity; and C is the correction factor for a threshold of the amplitude level. Coefficients B and C are determined using the known methods.

The danger of cracking in the material of a structure under loading is evaluated using the analysis of the kinetics of the AE development, including the analysis of common data obtained at the stages of holding the structure under loading. To compare and generalize the results regardless of dimension the analyzed parameters are normalized to unit:

$$\bar{E}H = f(\bar{P}), \tag{6.21}$$

where $\bar{E}H = E_i/E_{i\max}$; $\bar{P} = P_i/P_{i\max}$; E_i is the energy accumulation of the AE signals while holding a specimen under loading in the selected time interval; P_i is the load of the structure investigated; $E_{i\max}$ is the maximal value of the energy accumulation of the AE signals while holding a specimen under loading in the selected time intervals; $P_{i\max}$ is the maximal load of a structure during testings. The experimental data are analyzed with approximation as described above, using the equation

$$\bar{E}_H = a\bar{P}^b, \quad \text{at } t_i = \text{const}, \tag{6.22}$$

where a, b are the constants. The absolute value of the power index $b < 3$ proves that the defects that develop in the material of a structure are not dangerous in this case.

Classification of the AE sources by the degree of their danger. Additionally, the results of AE testing can be represented as a list of the recorded AE sources that belong to a certain group depending on the value of the AE parameters. Such evaluation is done for every AE source, while the state of the investigated structure is evaluated by the AE sources of a certain type. The choice of a particular system of the AE source classification and the criteria for assessing the state of an object depends on the mechanical properties of the material of an IO. The classification system and the assessment criteria of the structures' state are chosen using the classification systems, and the criteria for assessing the state of a structure of IO state are given below.

The admissible level of the AE source generation in a fracture is established while preparing a particular structure for AE diagnostics in accordance with existing methods. The AE sources are classified by the following AES parameters: cumulative count, number of pulses, amplitude or amplitude distribution, energy or energy parameter, count rate, activity, and concentration of the AE sources. The system of classification also includes the parameters of loading the tested structure as well as time parameters.

By analogy with approaches [12, 13], the revealed AE sources were divided into four groups: Group I—passive; II—active; III—critically active; IV—catastrophically active. The choice of the classification system of the AE sources and of a possible level (group) of sources is performed each time during AE diagnostics of a particular structure. Every superior group number of the AE source requires a fulfillment of all actions stated for the sources of an inferior group number. A final assessment of admissible AE sources, while applying additional types of non-destructive testing is performed, with the use of defect parameters found by linear fracture mechanics methods, strength calculation methods and other operating standards.

Amplitude criterion. An average amplitude A_{av} of at least three pulses with the individual amplitude A_c is determined for each AE source for the selected observation period. The amplitude is corrected, taking into account the AES damping during their propagation in a material.

The maximum value of an admissible amplitude A_t was determined in the previous experiments:

$$A_t = B_1 \times U_{th} + B_2 \times A_c, \tag{6.23}$$

where U_{th} is the threshold value of amplitude level; A_c is the value of the AE signal exceeding the threshold value that corresponds to the crack growth in a material; and B_1 and B_2 are the coefficients determined within the range of 0…1 from preliminary experiments.

The sources are classified as follows: Group I includes a source for which the average amplitude of pulses was not calculated (less than three pulses are obtained

during the observation interval); Group II—the inequality $A_{av} < A_t$ is satisfied; Group III—the inequality $A_{av} > A_t$ is satisfied; and Group IV—a source that includes at least three recorded pulses, for which the inequality $A_{av} \gg A$ is satisfied.

Specific values of A_t, B_1, and B_2 depend on the material of a structure and are determined in the preliminary experiments.

Integral criterion. For every area, the activity F of the sources of AE signals is calculated using the following expression:

$$F = \frac{1}{K}\sum_{k=1}^{k}\frac{N_{k+1}}{N_k}, \tag{6.24}$$

where

$$\frac{N_{k+1}}{N_k} = \begin{cases} 1 & \text{at } N_k = 0 \quad \text{i} \quad N_{k+1} > 0 \\ 0 & \text{at } N_k > 0 \quad \text{i} \quad N_{k+1} = 0 \end{cases}, \quad k = 1, 2, \ldots, K. \tag{6.25}$$

Here, N_k is the number of events throughout the k-th interval of parameter estimation; N_{k+1} is the number of events throughout the $k + 1$-th interval of parameter estimation; k is the number of intervals of parameter estimation. The observation interval is divided into k intervals of parameter estimation. Estimation of the criterion was done taking into account the dependencies: $F \ll 1$, $F = 1$ and $F > 1$.

Throughout each recording interval, a relative force J_k of the AE source was determined as follows:

$$J_k = A_K \Big/ W\sum\nolimits_{k=1}^{K} A_k, \tag{6.26}$$

where A_k is the average amplitude of the source throughout the interval k; A_K is the average amplitude of all AE sources throughout whole object except for that analyzed for interval k, and W is the coefficient determined in the preliminary experiments.

Local-dynamic criterion. To estimate this criterion in real time, the following AE parameters were used: N_{i+1} is the number of AE pulses in the successive event and N_i is the number of pulses in the preceding event, or: E_{i+1} is the energy of the successive AE event and E_i is the energy of the preceding AE event.

The parameter U^2, which is the square of AES amplitude, can be used instead of energy. For every event, the values W_{i+1} and V_{i+1} are calculated using the following expressions: $W_{i+1} = N_{i+1}/N_i$, or $W_{i+1} = E_{i+1}/E_i$,

$$V_{i+1} = \left(1 + \frac{P_{i+1} - P_i}{P_{i+1}}\right)^4 - 1, \tag{6.27}$$

where P_{i+1} is the external parameter value at the moment of the successive event recording (if time is used as a parameter, then it is an interval of time from the beginning of an observation interval); P_i is the external parameter value at the moment of the preceding event recording (if time is used as a parameter, then it is an interval of time from the beginning of an observation interval). Sources were classified as follows: Group I—$W_{i+1} \leq V_{I+1}$; Group II—$W_{i+1} = V_{i+1}$; Group III—$W_{i+1} > V_{i+1}$; Group IV—$W_{i+1} \gg V_{i+1}$. During testings, an on-line recording of information and processing of the AE data were done. After NDT of an object, data were analyzed and processed by a personal computer that was included in the AE testing system.

6.6.3 Results of the AE Testing and Their Interpretation

During hydraulic testing in the first and the second stages (external and internal reservoirs), a moment of abrupt increase of the AES amplitude was recorded. Using technical means, a criterion was evaluated that indicated the appearance of fracture in the place of a stripping hatch welding. Having adopted certain decisions, agents of corresponding services made a visual observation of the indicated place of the AES generation. As a result, the defect was detected, which after testing by other NDT methods caused the halt of the process of filling the reservoir with water and hatch replacement.

After that, according to the schedule of the reservoir filling with water, the AE testing was continued. At a mark of +13.94 m, the AES were within the limits of the background level. During the subsequent reservoir filling above the mark +13.95 m, the AE intensity increase was recorded (Fig. 6.24a, b). This process was observed up to the mark of +13.97 m of the reservoir filling (Fig. 6.24c, d). The recorded increase of the AE intensity lasted 45 min. After the water supply was stopped, additional inspections and corresponding consultations permitted ascertaining that this increase was caused by an abrupt increase in the water supply rate to the reservoir (to 1000 m^3/h), which affected the background level of the AE signals. When the rate of the water supply decreased to the previous level (500 m^3/h), the recorded AE signals were within the limits of the previous safe background level.

During an internal filling of the reservoir with water, the AES that did not exceed the background level were observed. The processing of the AES using the established criteria showed that they belong to the Group I sources, i.e., passive ones, which under continuous monitoring did not show a tendency towards defect development, although at certain moments, a single, non-dangerous growth of the AES intensity was recorded. At the +17.62 and +18.39 m marks, the AES were also recorded with somewhat higher energy and were classified as Group II sources.

The results of processing the AE signals of higher intensity using the integral and local-dynamic criteria are presented in Table 6.7.

Thus, the results of the AE tests showed that the growth of the intensity of AE signals at certain moments of loading was caused by the following technological

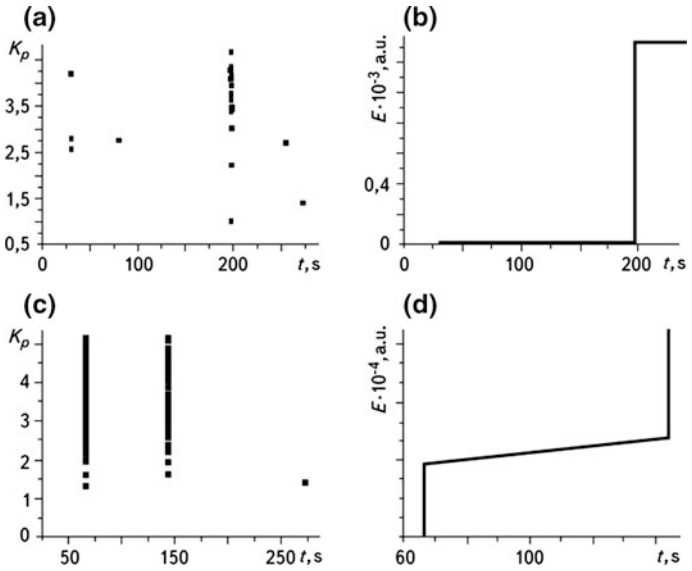

Fig. 6.24 Time variation of the factor K_p (**a**, **b**) and the AES energy (**c**, **d**) during reservoir filling from the +13.94 to +13.95 m mark (**a**, **b**) and from the +13.95 to +13.96 m mark (**c**, **d**)

Table 6.7 Classification of the recorded AE sources

Period of AE signals recording	Number of sources by groups											
	Integral criterion ($W = 0.1$)				Integral criterion ($W = 0.01$)				Local-dynamic criterion			
	I	II	III	IV	I	II	III	IV	I	II	III	IV
External reservoir	0	10	4	0	6	8	0	0	3	2	8	0
Internal reservoir 20–24 days	0	9	0	0	2	7	0	0	0	1	0	0
24–27 days	0	41	0	0	12	29	0	0	–	–	–	–
27–29 days	0	31	0	0	11	20	0	0	–	–	–	–
29–33 days	0	0	0	0	0	0	0	0	0	0	0	0

factors: the presence of cracks propagating under loading, an increase in the rate of water supply, and stress relaxation in the reservoir walls. In the material that was not likely to fail, the AES parameters did not exceed the background level at all stages of loading.

6.7 AE Testing and Diagnostics of Building Structures

The earliest information on the efficiency of using the AE method for industrial inspection and diagnostics of building structures in operation appeared in the late 1960s [39–42]. The method was intensively developed and improved, which is evidenced in the papers that were published. According to the data [43], already in the USA in the 1970s, the national standards for inspection and NDT of bridges using the AES were developed and have been widely used ever since. These standards require inspecting bridges at least once every two years. Earlier, the visualization of defects of foundations and elements of their lower constructions was performed using submarine cameras. However, it was not always possible to reveal the cracks. Therefore, in such cases, even slight defects caused the failure of bridges. For example, a 3 mm-long crack caused a catastrophe at the Pleasant Bridge; the Silver Bridge failed because of a defect of less than 4 mm, and the Mello-Mild Bridge failed due to the presence of fatigue cracks after 12 years of use.

For reinforced concrete bridges of large weight and rigidity, there is only a slight probability of the appearance of irreversible damages due to the presence of fatigue cracks. In such structures, corrosion of a preliminarily stressed reinforcement turns out to be more dangerous. Besides, it is much more difficult to detect defects in reinforced concrete. Proceedings from the above-discussed, now- effective NDT methods are being intensively developed all over the world, and these methods are based on various approaches. However, the methods that use the AE phenomenon are preferable. For example, in Japan in the 1970s, the integrity of old and new railway bridges, local railways, runways, impacting equipment and hoisting cranes began to be checked using these methods [44]. In particular, a four-year AE checking of the runways in airports showed that there is a correlation between the processes of crack propagation, loading, and AES. In [45], the AE and micro-seismic research into the estimation of the methods for testing the growth of damage in the coatings of the same runways is described. The data collected enabled comparing the accuracy of the methods of the AE sources' location, i.e., time-related, zonal, and impact-successive. It has been shown that the last two methods are potentially more accurate than a time-related method. In practice, they provide a satisfactory accuracy of the active areas' location, and it is noted that in the conditions of high damping, an impact-successive method provides the best accuracy. Gradually, the AE method gained more and more recognition, and already in July 1979, information on more than 100 industrial inspections of various structures (bridges, cranes, etc.) with the use of the AE phenomenon was published [46]. About 20 of these structures were at the stage of being assembled, 90 were in the process of current operation, and more than 10 objects were inspected in in-service conditions.

A wide application of reinforced structures in transport building, especially for building bridges, requires corresponding NDT facilities both in the process of work execution and during exploitation. A detailed analysis of the failures of reinforced

concrete bridges shows that in the process of construction, a principal cause of failure is the violation of the regularities and technologies of the work performed, while in exploitation there are cracks in structures, primarily due to the action of corrosion of products of a pre-stressed reinforcement. Therefore, alongside traditional methods of NDT of reinforced concrete products, the AE method has also been more widely used lately. Such studies are actual today, which is evidenced by publications in scientific literature. In particular, in [47] the authors showed that in the process of bridge exploitation under dynamic loading, background noise is formed causing a distortion in the AES frequency spectrum. Analytical dependencies are presented therein for obtaining a formula for the calculation of the maximal size of the bridge tested area as well as a method that is described for selecting the optimum working frequency band of AE equipment when distortions of the AES spectrum are minimal.

The paper presents the results of the calculation of normalized AES spectra in three characteristic regions of a metal bridge: 1—with a fatigue crack; 2—unfit riveted joint; 3—non-damaged structural element. The spectra differ both by the level of power and by the shape that can serve as a criterion for characteristics of damages in bridges. In paper [48], the use of the AES spectral analysis is considered to be a reliable method of corrosion cracking and crack propagation detection. Here, the information on the methods of the AES processing based on the application of the fast Fourier transform, as well as the charts of the design of an automated AE diagnostics system are presented. The efficiency of this approach is evidenced by the results obtained in [49], and by the AE testing of reinforced concrete bridge structures. The results of the AE inspection of 36 railway bridges are also described in [50], where some suggestions for the improvement of the AE test procedure and data processing are presented.

The results of experimental studies on the relationship between the AE parameters and cracks in the elements of reinforced concrete bridges under loading and under the action of corrosion products are discussed in [51]. Experimental data on the determination of noises in a reinforced concrete bridge in the conditions of intensive motion of electric vehicles are also discussed. Their classification is given, and the physical processes of initiation and methods of AES extraction from them are considered. The experiments were conducted using the AE analyzers of the AVN-1M and AVN-3 type.

Using a movable multi-channel laboratory for the AE diagnostics, an inspection of the Crimean, Velyko Kamianyi, and Velyko Ustynivskyj bridges, and a metro bridge in Luzhnyky was carried out [52]. The inspection was done in order to assess a bearing strength of structures and their lifespans, to detect potentially dangerous defects, the uniformity of distribution of stresses on bearing units and elements, to predict crack growth resistance of materials, and to study the effect of climatic and other factors on the dynamics of load redistribution. The analysis of the dynamics of the development of AE generation processes in real time and a correlation analysis of distribution permitted, in accordance with the developed criteria, detecting the highly dangerous areas, to localize the areas with defects, and to estimate the local stress state in bearing elements. In paper [53], the authors based

on the laboratory research on fracture of a concrete with plasticizer additives elaborated, a method which, they believe, can be used to estimate the quality of a roadbed.

In the 1970s, investigations aimed at using the AE method for assessing the integrity of beam-and-girder constructions began in the U.K. [54]. They were initiated by the Committee for Construction, following the failures of these structures made of a pre-stressed concrete. The NDT of these products by conventional methods did not yield satisfactory results, and the AE method, in the authors' opinion, was most effective for this purpose. This statement was scientifically grounded in paper [55], presenting the results of the experiments on pre-stressed pressure vessels made of concrete and on casings of nuclear reactors in the USA by AE inspection and NDT. The AE phenomenon was used together with radiographic and ultrasonic NDT techniques.

Cracks are formed in large-panel-bearing elements of buildings in the process of their manufacture, transportation, stocking, and mounting. These cracks are mainly from temperature shrink and a force-induced nature. Force-induced cracks are very dangerous for structure operation because they propagate due to the applied loads, considerably violate the conditions of structure exploitation, create emergencies, and lower the reliability and lifespans of buildings. To estimate the effect of cracks on the strength-bearing of a structure, it is necessary to determine not only their origination but also the character of their development under loading. Therefore, in this case, the AE method turns out to be very efficient for determining the degree of danger of force-induced cracking in structures. On the other hand, to arrive at a well-grounded conclusion about the state of a cracking structure, it is necessary to observe the structure for a long period of time, and to collect and analyze statistical data on the crack propagation dynamics and crack parameters during the early years of object exploitation.

In [56], the crack initiation in bearing structures was inspected in the following way: In a structure with cracks, and in a similar one without cracks, both of which were subjected to identical loading (on the same floor of a building), the number of AE pulses was recorded at a discrete increase of a load due to the assembling of the next floor structures. Using the results of AE testing in the structures with defects and in those free of defects during an increase of the load up to the calculated value, empiric dependencies of the number of AE pulses on the level of a load were built, as well as time series of the number of pulses for all the values of the second. The results of testing the state of bearing wall panels having force-induced cracks, testified to an available discrepancy between the designed operation conditions of structures and their real service conditions. It was shown that an increase of the rigidity of buildings with the growth of the number of stories, obviously, resulted in a considerable and more uniform redistribution of forces and slowed down the propagation of cracks. Therefore, structure-strengthening measures were not always justified. This was proved by the results of durable AE observations of cracks during the first two years of exploitation that showed the invariability of crack parameters. As a result of the AE research, the method of estimation of crack

formation in reinforced concrete structures using the AES was developed and put into practice.

The AES in mountain rocks during cement solution pressurization into a dam was analyzed in paper [57], where highly promising economic capabilities of the AE method for diagnosing the state of such buildings were confirmed. A similar result was obtained by the authors [58], where a possibility of applying the AE for inspection of the bearing strength of frozen foundations during their defrosting was considered. The method for laboratory and field testing was described, and the test results were presented. The possibilities of integrating various diagnostic systems were considered as well.

The problem of utilizing the AE phenomenon for estimating the displacement of soils and for the development of displacement prevention measures was comprehensively discussed in [59]. The results of both laboratory and field studies were presented. The pertinent data of such experimental testing published by scientists from many countries were analyzed, and the positive results showed good prospects for using the AE method, its high resolution and information capacity, and its advantages as a technique for predicting of the state of the objects tested, such as buildings and structures.

6.8 The AE Inspection of Bridges in Ukraine

Bridges form only a minor part of the total length of transport communications, but their technical condition affects the transportation safety to a great extent. This is conditioned by the fact that bridges concentrate traffic and it is more difficult to provide their reliable and durable operation compared to roads, because they are more complicated engineering structures and are subjected to the action of various loadings and effects [60]. Apart from the action of transport loading and their own weight, span bridge structures are subjected to dynamic wind effects and longitudinal loadings during the braking or acceleration of vehicles, etc. Bridge footings are also subjected to an additional pressure of ice, the impacts of floating materials, and in earthquake-prone regions.

There is a wide network of motor roads and railways in Ukraine; it includes 16,300 road-transport national and 358 km long local bridges, 4082 communal bridges that are 184.8 km long, and 8050 railway bridges that are 210.4 km in length [61]. Many bridges that have damage and defects are in use in Ukraine. Data of large-scale inspections of the bridges carried out by various organizations in the 1980s stated that [62, 63] bearing structures mainly contain the following defects: fracture of protective coatings and corrosion of steel bridges—41% of the inspected bridges; splitting off, cavities, and cracks in a concrete—65%; corrosion of reinforcement—40%; and carbonization of a concrete protective layer—60%. The actual lifespan of reinforced concrete bridge structures is 25…30 years, at which point the necessary expensive repair work does not promote the potential properties

of reinforced concrete as a material [64]. The principal causes of this are the corrosion of reinforcement and concrete.

Bridge constructions have a tendency to brittle fracture, i.e., to fracture by propagation of crack-like defects. The fracture process in such materials is not immediate because some time passes from the moment of crack initiation to the beginning of reaching its critical value. Therefore, the early detection of such defects and estimation of sub-critical crack growth stages is an important scientific and technological problem. It is difficult to detect a considerable part of defects in bridges because their metallic elements are covered with paint, the reinforcement is inside the concrete in reinforced concrete structures, and crack initiation and propagation often occur inside the material. Thus the problem of providing a reliable and long-term exploitation of bridges becomes more and more urgent because the ages of the bridges increase, the weight, intensity of motion and dynamic effects on the bridge structures grow, and the aggressiveness of the environment increases. The growing complications in providing a reliable and durable exploitation of bridges require new approaches to their technical diagnosing [65].

To estimate a macro-crack initiation in bridge structures by means of the AE method, an approach proposed in [66] is used. It consists of using the estimation criterion K_{pj} which is based on the rate of the recorded variation of the AES energy density.

$$K_{pj} = \lg\left(E_j/\tau_j^2\right), \tag{6.28}$$

where

$$E_j \text{ is the } j-th \text{ AES energy; } \tau_j \text{ is its duration.}$$

In order to digitally process the AES, expression (6.28) was transformed into:

$$K_{pj} = \lg\left[\sum_{i=1}^{n} (A_{ji})^2/\mathrm{LE}_j^2\right] + \lg(\Delta U^2/\Delta t), \tag{6.29}$$

where Δt is the time interval of the AES sampling (Δt = const); A_{ji} is the number of bits of an analog-digital converter for the i-th sampling of the j-th AES amplitude; n is the number of amplitude counts for the j-th AES; and LE_j is the j-th AES duration ($\mathrm{LE}_j = n$).

If the sensitivity of the AE equipment ΔU and sampling frequencies of the input signal are set, the second part of equation (6.29) becomes constant B, that is

$$K_{pj} = \lg\left[\sum_{i=1}^{n} (A_{ji})^2/LE_j^2\right] + B. \tag{6.30}$$

The AE *inspection of the bridge across the Western Bug River.* An object under investigation was the bridge roadway near the village of Yahodyn in the Volyn Oblast. The bridge was built in 1953–1954 from metallic structures taken from the demountable bridge built in the 1930s. The bridge is of a split-type with three spans, and its cross-section consists of two girders according to a 3×62 m scheme. The size of the bridge roadway is G-7.0 + 2×1.55 m. Metallic girders are riveted with parallel bridge booms with a carriageway on the bottom and triangular grillwork. The distance between the axes of girders is 8.65 m, and top and bottom booms are of an H-like cross-section. Diagonal webs are of an assembled, double-T, through and grated type. The assembled buckstays are also of a box-like cross-section, and there are horizontal crossing connections in the plane of the top and bottom bridge booms. The bridge roadway is made of monolithic reinforced concrete arranged on metallic sections. It lies on a beam cage made of cross-beams of variable cross-sections that are fastened to the girder joints, and longitudinal double—T beams fastened to the supports of cross beams. The coating of the bridge roadway is asphalt-concrete, without coating on the sidewalks. Bridge supports made of concrete are massive and are located on reinforced concrete hanging piles. Unmovable supports are made of metal with top and bottom equalizers and a cylinder hinge between them, while movable supports are metallic roll bearings.

The span structures of the bridge were subjected to static and dynamic loadings. All three spans were loaded alternately by trailer trucks weighing from 200 to 380 kN each. The "AKEM" programming complex recorded the AES.

Static loading was applied as follows: Trailer trucks drove successively to the roadway of every bridge span (Fig. 6.25) and then stopped. The trucks weighed 200…380 kN, and there were a maximum of eight trucks on the span roadway. After the arrival and stopping of every truck, the AES were recorded and processed. At the same time, the bending of girders in the middle of a span was measured with a deflectometer, while strains of the most stressed girder elements were measured with electromechanical strain gauges.

The AE data were recorded for 45…120 s, and the AET was mounted in the region of maximum tensile stresses (a middle part of the span; see Fig. 6.26). Bridge spans were numbered, beginning in Ukranian territory. Before mounting the AETs on a bearing beam and a stiffening rib, they were cleaned of paint and rust; the diameter of the cleaned surface area was about 20 mm. After applying an acoustic transparent contact layer, the AETs were pressed to the metal surface by clamps.

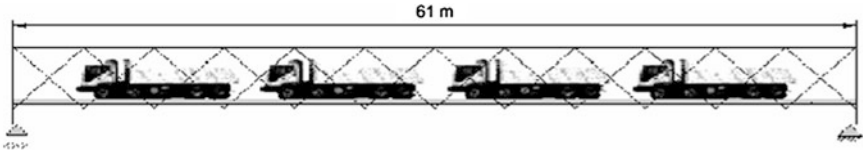

Fig. 6.25 Static loading on the bridge span

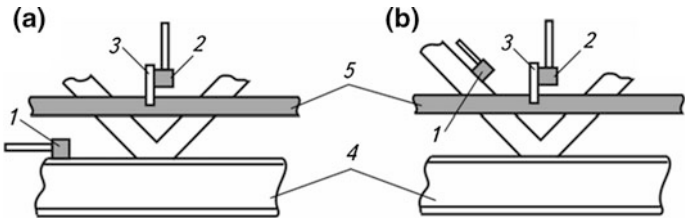

Fig. 6.26 Location of the AET under the loading of span 0–1 (**a**) and spans 1–2 and 2–3 (**b**): *1* is AET No. 1; *2* is AET No. 2; *3* is a waveguide; *4* is a lower girder boom; *5* is a reinforced concrete plate of the bridge roadway

While testing all bridge spans, AET No. 2 was located on the waveguide placed directly in the concrete. The waveguide was made from a reinforced rod of 8 mm in diameter and 150 mm long. On one of the edges of the waveguide, parallel to its axis, the flat of a depth of 4…3 mm was made in order to mount the AET. The waveguide was inserted into a hole (7 mm in diameter, 10–15 mm deep), which was drilled into the concrete. The AET was mounted on the waveguide with tension, and two channels were simultaneously recording and processing the AES.

During the first kind of dynamic test, one truck with a fixed weight was driven at a constant speed of 5, 10, 20, and 40 km/h along each bridge span. The recording and processing of AES began at the moment the trailer truck arrived at a span, and ended when it drove away from the bridge span. During the second kind of dynamic test, the truck crossed a barrier placed in the central part of the bridge span. The weight of the truck was fixed, and the speed was the same as for the first type. A 10 cm. thick wooden square beam was used as a barrier.

The criteria estimation of the detected AE signals caused by cracks was performed in accordance with a crack evaluation by the K_p factor. For instance, at the first, second, and fourth loading degrees of span 0–1 with one, two, and three trucks, respectively, crack propagation was not detected. The AES caused by cracks were recorded only at the fourth stage of loading (four trucks). The analysis of the recorded AES parameters (amplitude, energy, duration) shows that they are of low magnitude, which testifies to the stabilization of the development of micro-processes in the material of a structure. Further testing of the bridge using the AE method showed that under service loadings, no defects whose growth would endanger the span structures appeared [65].

The AE inspection of the road-transport bridge across the Pivdennyi Buh River [67]. A bridge is located near the village of Lupolove on the Kiev-Odessa highway. The span structure of the bridge is made of non-cut steel iron concrete, made according to the scheme (32.9 + 43.3 + 43.3 + 32.9 m), and it consists of six main metallic beams joined by a monolithic reinforced concrete plate of the bridge roadway and constraints. The width clearance of the bridge includes a 3-meter dividing strip, a 7.5 m wide dual roadway, 2 m thick safety bands, and a 0.78 m wide sidewalk. The total bridge width is 14.14–153.3 m long, and a facade-building

Fig. 6.27 General view of the bridge during testing

height is 2.1 m. There are tower-shaped intermediate supports made of reinforced concrete (Fig. 6.27).

The bridge span structure was subjected to static and dynamic loadings. Trucks weighing 250 kN each were used as a test load. AE signals were recorded and processed by means of an "AKEM" programming complex [66]. The aim of the research was to detect the AE sources related to the defects that are active under static and dynamic loadings of bridge structures, as well as to reveal the regularities of the AE process.

A maximal bending moment was formed in a span 3–4, and the AET was placed on the rib of the upright dual-T metallic beam (Fig. 6.28b) in accordance with the loading Mode 1. The following two modes (Nos. 2 and 3) enabled creating maximal forces in the reinforced concrete cantilever of a roadway plate, and the AET was mounted on the concrete (Fig. 6.28c). Before placing the AET on the metal, the paint was cleaned from its surface; after this, a layer of "Ramzay" acoustic-transparent filler was applied and the AET was pressed to the surface by clamps. The AET was pressed to the concrete by a magnet that was fixed by its one end to the AET, and the other end was fixed to the metal of the dual-T beam top shelf (Fig. 6.29).

During static testing, the AES recording began at the moment the trucks stopped in the places determined by the testing modes, and the data were recorded for 40… 60 s. During dynamic tests, the AE was recorded from the moment of the arrival of the trucks at the bridge up to the moment of their leaving it. The AET location was similar to that for static testing according to Modes 2 and 3.

The criterial assessment of detection of the AE signals caused by cracks was processed, as shown above, by means of the K_p factor. When the AET was placed on the metal surface, the value of the criterion for extraction of the AES caused by cracks (the K_p factor) was assumed to be 3, and for concrete it was 6. The AE sources that were revealed, as described above, were divided into four classes:

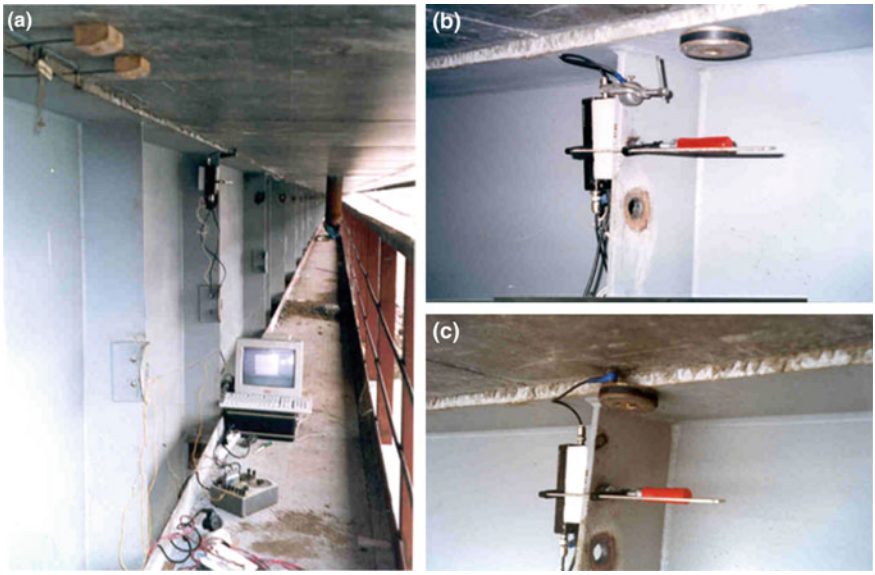

Fig. 6.28 The AE "AKEM" equipment (**a**) and methods of mounting the AET on metal (**b**) and concrete (**c**)

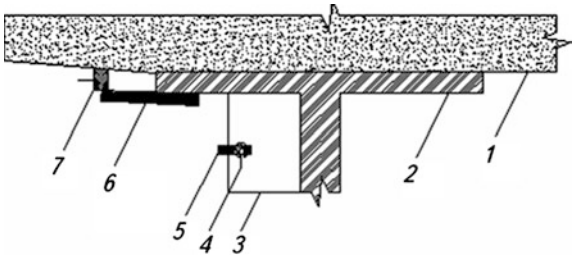

Fig. 6.29 The AET location during bridge testing: *1* is a reinforced concrete roadway plate; *2* is a metallic beam; *3* is a metallic beam edge; *4* is the AET placed on metal; *5* is a pressing clamp; *6* is a magnet; *7* is the AET placed on concrete (Modes *2* and *3*)

Class I is a passive source; II, an active source; III, a critically active source; and IV, a catastrophically active source.

Using the integral criterion, which was also described above, the AE sources' activity was calculated from the expression:

$$\tilde{A} = a\widetilde{\Pi}^{b}, \quad \text{at } t_i = \text{const}, \tag{6.31}$$

where $\widetilde{A} = A_{\mathrm{T}}/A_{\max}$; $\widetilde{\Pi} = \Pi_{\mathrm{T}}/\Pi_{\max}$; A_T, $\Pi_{\max}$ are the current and maximal values of parameters. The absolute value of the power index $b < 3$ proves that the defects that develop in the material of a structure are not dangerous.

Under the static testing of the bridge span structure by Mode 1, the AES from the defects in the metallic beam material were recorded. This is confirmed by the

corresponding values of the K_p parameter. The analysis concerning the development of dangerous defects in the material structure under the loading of the span showed the following: A relationship between the load level and the accumulated AE energy is observed beginning at the 12th second. In this case, the values of coefficients in the approximating expression are as follows: $a = 0.0878$; $b = -1.76897$; $\sigma^2 = 0.02824$. The absolute value of the power index is $b < 3$, and while loading the bridge span structure by Mode 1, the defects that develop in the structure of a material are not dangerous.

Under the static testing of the bridge span structure by Modes 2 and 3, the AES caused by micro-cracks in the reinforced concrete plate of the bridge roadway are recorded, which is proved by the corresponding values of the K_p parameter that do not exceed 6. The following was shown by analyzing the development of dangerous defects: Under the loading Mode 2, beginning at the 20th second, a relationship between the accumulated AES energy, and the load of a span was observed. The analysis of the relationship using data formalization shows that it can be described by the expression with the parameters of approximation: $a = 0.26273$; $b = 0.05307$; $\sigma^2 = 0.36816$. Under loading by Mode 3, the dependence between the accumulated AES energy and the loading of a span appeared after 7 s. After 11 s: $a = 1.08086$; $b = 1.61458$; $\sigma^2 = 0.04489$. The absolute value of power index is $b < 3$, i.e., during the bridge span structure testing by loading Modes 2 and 3, the defects that develop in the material structure turned out not to be dangerous.

Thus, bridge testing using the AE method showed that there are no dangerous defects in the bridge structure that could hinder a reliable and safe use of span structures. Moreover, these defects did not show any tendency to develop. It is recommended that such tests be repeatedly performed after a certain period of time in order to estimate the state of the bridge span structures and to create a system of their monitoring. This would permit developing a database for establishing the dependencies used to estimate the bridge lifespan according to the AES parameters.

The AE inspection of the bridge across the Prut River in Chernivtsi. This bridge is located on the main highway of the third category M20 Zhytomyr–Chernivtsi–Terebleche (Fig. 6.30 [68]). The bridge is made of metal, has 6 spans, and was built according to a chart: 38.60 + (39.14 + 2 × 38.90 + 39.14) + 38.60. The bridge is 247.18 m long.

A permanent bridge passage with metallic span structures on rubble concrete footings was built in 1927–1931 and crossed the Prut River at a right angle. During the World War II the bridge was destroyed twice and rebuilt twice. The foundation of the footing 2 was not destroyed and a 5-m high primary rubble concrete footing was built on it. A temporal frame bricked with its basis in rubble concrete was arranged over it; the bridge girders were supported by a metallic frame through a grillage foundation. In 1961 a wooden roadway of the bridge was replaced with reinforced concrete.

The span structures consist of two through metallic girders with parallel booms and a carriageway on the bottom boom. Girders are of an open type and do not have wind constraints on the upper boom. The filling is constructed as a triangular web with additional vertical tower bodies.

Fig. 6.30 A general view of the bridge across the Prut River in Chernivtsi

Coastal spans 0–1 and 5–6 are covered with cut girders. The river bed spans 1–2…4–5 are covered with a non-cut, four-span girder. Every span girder is divided into 10 panels (3.8–3.87 m long). In a transversal cross-section, the distance between the axes of girders is 6.51 m, and their height is 4.04 m.

The sections of girder elements are made of the rolled elements of channels and angle bars that are reinforced on the top and on the bottom booms by metallic sheets in the middle panels and in the supporting areas of non-cut girders. In a transversal direction, the rigidity of span structures is provided by horizontal diagonal connections of angle bars (2*L* 90 × 90 × 10 mm) located at the bridge boom bottom level.

Abutment spans are made of rubble concrete and are monolithic with undersides. Supports consist of two parts and end with cornices. The lower part is widened, and its height is about 5.0 m, with the top part about 1.5 m high. A reinforced concrete underside is made as a monolith with sidewalk cantilevers about 7 m long. Two concrete diaphragms are mounted on the bottom of sidewalk cantilevers at the up-river bridge side and at the down-river side.

Intermediate supports are rubble concrete, hollow (except for the restored support 2), slush plastered, and made of two parts: The lateral sides of the bottom parts of intermediate supports have inclinations with a ratio of 15:1. The up-river bridge side is executed as an elongated ellipse and acts as a breaker; the down-river bridge is semi-circular. Foundations of all supports are caissons laid 20…35 m deep. Girders are set on the supporting mobile (bowled, rolled) and immobile (balance) parts.

The reinforced concrete plate of a bridge roadway is an assembled structure 11 cm thick; its cross-section is a trapezoid that consists of two Γ-shaped units. A longitudinal weld is located along the axis of the bridge roadway. The length of a

unit is equal to the plate length, and transversal welds are located over the crossbars. The plate is placed on a beam cage that consists of longitudinal and transversal beams.

Transversal beams are assembled, riveted from angle bars and double-T sheets 0.74 cm high, have a calculated length of 6.15 m, and are installed in every joint of a bottom boom. They are tightly joined with the support of the main girders and form a semi-frame. Two stiffeners made of 90 × 90 × 10 mm angle bars are riveted to the vertical ribs on both sides to provide local stability.

Longitudinal beams are made of an I-bar 30 and are tightly connected at one level (by a supporting table) with crossbars. Six longitudinal bars are placed in the transversal section with an axes distance of 1.0 m and an estimated length of 3.7… 3.75 m. A plate is set on the bar cage using reinforced concrete square beams of a 13.5 × 12.5 cm cross-section, made as a concrete monolith with the top boom of the longitudinal beam. The length of the squared beams is equal to the length of the panel.

Sidewalks are placed on the external bearing-out cantilevers made of a rolled metal (angular bar and a channel) that are riveted to the girder parts. The channels are inlaid in a cantilever, on which corrugated iron flooring is placed. The space between the girder elements is covered by a metallic sheet. Communications facilities are laid under the flooring of sidewalks.

A coating is applied over the bridge roadway that consists of a flashing, draining triangle, and a 7 cm. thick layer of asphalt concrete. The roadway is protected by a 0.75 m high metallic barrier.

The bridge railing is metallic, riveted, and specially designed. On the underside walls of a support 10, the railing is reinforced with concrete parapets. On support 6, the railing is metallic, and mounted on sidewalk blocks. On the up-river side of the bridge, the light towers made of metallic cone-shaped pipes are mounted. Over supports 0, 1, 5, and 6, deformation welds are covered with sliding metallic sheets at the level of a coating.

Under a static loading of the bridge 13, the modes of sequential loading of all girders were realized. As a test loading, two tipper “KrAZ” trucks were used, loaded with ballast weighing 270 kN each (Fig. 6.31). The deflections (vertical displacement) were measured in the middle part of girders 0–1, 1–2, and 5–6 by drum-gear deflectometer PAO-6 of the Aistov system; stresses (relative deformations)—in the middle of girders 0–1, 1–2, 5–6 at the top and bottom shelves of the main bars—were measured by Aistov electromechanical strain gauges, and micro-indicators with a 200 mm base.

The bridge was dynamically loaded by the “KrAZ” tipper trucks with a ballast that was moving at various speeds on the bridge roadway, having passed the barrier made of a wooden squared beam of the 10 × 10 cm cross-section, stopped and were unmovable across the middle of a girder. The following loads were realized: one “KrAZ” tipper truck was driven at speeds of 10, 20, 30 km/h in the direction from support 6; another “KrAZ” truck moved across the 10 × 10 cm barrier at 20 km/h.

Fig. 6.31 Loading the bridge span 1–2 by two "KrAZ" tipper trucks

Under all modes of dynamic and statistic loadings, the AES were recorded from bearing structures of the bridge, as in previous cases, using the "AKEM" program complex that was designed for a personal computer that used "PCLabCard" technology. To evaluate the dynamic characteristics, there a VIBROPORT 30 device equipped with a computer produced by the "SCHENCK" company (Germany) was used. A vibration sensor was mounted on the top boom of the girder in the middle of the investigated bridge span (0–1, 1–2 and 5–6) [68].

The recording and analysis of AES during static testing began at the moment the truck stopped in the places determined by testing charts. Information was recorded for 40…60 s. The processing of the criterial estimates of the AES caused by cracks was also done using the K_p factor as in the aforementioned research.

As a result of static and dynamic testing of the bridge across the Prut River on the Zhytomyr–Chernivtsi highway, it was found that bridge structures do not contain defects and damage that could reduce their bearing capacity. To lengthen the lifespan of a bridge, it is necessary to finalize the studies on corrosion protection of metallic structures of a bridge using modern technologies and materials and do the repairs of bridge supports by arranging protective iron concrete shirts. It is recommended to set the limit of the load carrying capacity of the bridge with a maximal admissible temporary load of up to 300 kN per one span.

6.9 Prospects for Further AE Application

Thus, as numerous published data show, the second half of the twentieth century gave an incentive to the development and application of the AE phenomenon for NDT and technical diagnostics of various products [35, 69, 70]. For instance,

already in 1965 the Aerojet-General Company (USA) under NASA contract performed hydrostatic testing of the casing of a SL-1 rocket engine with a diameter of 6.6 m produced by the Tiocol Company [35, 70]. Using the AE method, the moment of sub-critical crack initiation and propagation under pressure that constituted 56% of admissible value was detected. The method of triangulation made it possible to determine the fracture location with an accuracy of 305 mm. This promoted the application of the AE method in research on the strength characteristics of structural materials, their fracture and metal science problems, and consequently for the determination of the coordinates of developing defects [71]. Further research effectively used the methods of AE diagnosing for testing the state of wing crossbars in aircraft [72] and in other elements of aviation structures in which initiation and propagation of fatigue cracks is possible [73].

Progress in microelectronics and, especially, in the development of a theoretical basis of the AE method, urged further studies. Estimating the state of rocket engines by 52-channel AE equipment [74] showed that using the criterion approaches, the defects can be divided into three groups: (a) safe; (b) those that need inspection and study; and (c) obviously dangerous. Publications appeared where the AE method was effectively used for the quality control of rods [75, 76] under the action of temperature and mechanical loading [77–79], and in gas flows [80]. The AE methods for determining the characteristics of structural materials, especially their crack growth resistance [81, 82], for locating the defects [83, 84], for determining their orientation [85], especially during exploitation of the objects [86], are still urgent.

Paper [87] describes the laboratory AE research of crack initiation from the holes for rivets under fatigue loading. The corrosion of rivets was accompanied by the AE that was recorded in the frequency band below 150 kHz. Therefore, the AE caused by fatigue fracture was recorded by the AET at the natural resonance frequency of 450 kHz. Basic information on the mechanisms of the fatigue fracture of rivets was obtained by amplitude distribution of the AES. Signals differ by a short time of amplitude growth, which is typical of crack growth. The distribution of the number of AE pulses vs. the number of loading cycles was calculated.

It is also shown there that there are other methods of utilizing the AE in diagnosing the state of structures and products. The most widespread are the methods of the AE inspection of leakages in vessels that operate under pressure [69–71, 87]. The Kaiser effect is most often used for this purpose, because the AES arise from the very start of a crack growth. They are recorded either during primary application of pressure in a vessel or under the repeated loading above the previously attained maximum level. During such tests, noises arising due to the leakage of liquids and gases from vessels give a substantial contribution to the recorded AES. Even at a slight leakage, the AE can be higher than the AE recorded during a crack growth. Therefore, in conditions of leakage detection by means of the AE, it is necessary to eliminate the leakage and then perform a subsequent AE testing of the object. The state of deep-diving into a submersible chamber was examined [87] using this method.

Pipelines and pipeline systems can be diagnosed using the AE method during hydrostatic testing by applying overpressure [88, 89]. The AET location depends on the thickness and diameter of a pipe, the type of protective layer, the composition of the soil (for an underground pipeline), the working environment in a pipeline, etc.

The wide use of the AE test methods for industrial equipment is also recognized [87], apart from those described in this monograph. Among them are the methods for assessing the state of the equipment for oil catalytic cracking, hydro-cracking, blast furnace, autoclave of pulp and paper production, mine fastening, cryogenic vessels for the storage of ammonia, spherical vessels, products of reinforced glass-fiber material, hydrolysis equipment, devices for hydrothermal treatment, absorption tower, materials of clock springs, surface coatings, quality of mechanical and heat treatment of components, and food, as well as honeycomb elements of airplane structures, buildings, geological processes, and others.

When analyzing the state and prospects of the development of studies using the AE phenomenon to estimate damaged products, it is necessary to distinguish between the following basic directions:

- Development of a theoretical basis in order to establish correlations between the AES parameters and the defects, and the elaboration of effective experimental methods for determining the crack growth resistance of structural materials;
- Creation and verification of new methods of detection of defects in structures during semi- or full-scale testing, which, in turn, use the results of theoretical and experimental research; and
- Development and production of new facilities for loading and for extracting the AE signals, as well as units for their processing in order to perform the NDT and technical diagnosing of the IO.

References

1. Webborn TJC, Stewens PG (1983) On-line monitoring by acoustic emission. In: 4th national conference on condition monitoring, London, 15–16 Mar 1983
2. Rogers LM, Monk RG (1983) In service monitoring of structural integrity by acoustic emission analysis. In: 2nd national conference on condition monitoring in the process industries, London, 10–11 May 1983
3. (1981) The EWGAE AE code for acoustic emission examination of sources of discrete acoustic events. NDT Int 14(8):181–183
4. Rogers LM (1978) Application of acoustic emission source location to on-line condition monitoring of fabrication, machinery and process plant. In: International physics conference on machine aided image analysis, Series No. 44, cr. 4., London, 5–8 Sept 1978
5. Rogers LM (1985) Measurement and interpretation of the acoustic emission from propagation cracks in steel structures. In: Proceeding of British Society for Strain Measurement: annual conference “structurual integrity.” Lancaster, 10–13 Sept 1984. Newcastle upon Tyne
6. Tuikin OP, Ivanov VI (1985) Faktornyy analiz ustoychivosti parametrov akusticheskoy emissii (Factor analysis of acoustic emission parameters stability). Defektoskopia 8:39–44

7. Johnson N, Lion F (1981) Statistika i planirovanie eksperimentov v technike i nauke. Metody planirovaniya eksperimenta (Statistics and planning of experiments in engineering and science. Methods of experiments planning). Moskva, Mir
8. Dunegan HL, Harris DO, Tatro CA (1968) Fracture analysis by use of acoustic emission. Eng Fract Mech 1(1):105–122
9. Ivanov VI, Belov VM (1981) Akustiko-emissionnyy kontrol' svarki i svarnych soedineniy (Acoustic emission testing of welding and welded joints). Mashinostroyeniye, Moskva
10. Ivanov VI, Bykov SP (1985) Klassifikaziya istochnikov akusticheskoy emissii (Classification of acoustic emission sources). Diagnostika i prognozirovanie razrusheniy svarnych konstrukziy (Diagn Predict Fail Welded Struct) 1:67–74
11. (1976) Standard recommended practice for acoustic emission monitoring of structures during controlled stimulation. ASTM E, pp 569–576
12. Watanabe T, Huchirizaki S, Arita HA (1978) Method of evolution the harmfulness of flaws in structures using acoustic emission techniques. The fourth acoustic emission symposium, Tokyo
13. (1980) Acoustic emission testing of spherical pressure vessel made of high tensile strength steel and classification of test results. NDIS 2412:6–8
14. Vald A (1960) Posledovatel'nyy analiz (Sequential analysis). Fizmatgiz, Moskva
15. Vakar KB (ed) Akusticheskaya emissiya i ee primenenie dlya nerazrushayuschego kontrolya v atomnoy energetike (Acoustic emission and its application for NDT in nuclear power engineering). Atomizdat, Moskva
16. Hutton PH, Kurtz RJ, Pappas RA (1984) AE/Flaw characterization for nuclear pressure vessels. In: Review of progress in quantitative nondestructive evaluation: proceedings of 10th annual review, Santa Crus, California, 7–12 Aug 1983
17. Hutton PH, Kurtz RJ (1985) Acoustic emission for on-line reactor monitoring. Results of intermediate vessel test monitoring and reactor hot functional. In: Review of progress in quantitative nondestructive evaluation: proceedings of 11th annual review, San Diego, California, 8–13 July 1984
18. Kuranov VN et al (1981) Ispol'zovanie metoda akusticheskoy emissii pri ozenke konstrukzionnoy prochnosti sosudov vysokogo davleniya i truboprovodov (Application of acoustic emission method in evaluation of structural strength of pressure vessels and pipelines). In: Trudy ZNIITMash (Proceedings of Central Research Institute of Engineering Technology (CNIITMash)), vol 165, pp 3–12
19. Troitskyi VA et al (1986) Nerazrushayuschiy kontrol' kachestva svarnych konstrukziy (Nondestructive testing of welded structures quality). Tekhnika, Kiev
20. Paton BY et al (1982) Perspektivy razvitiya kontrolya kachestva s ispol'zovaniem EVM pri proizvodstve svarnych trub bol'shogo diametra (Prospects of development of quality testing with the use of computer in production of welded pipes of large size). Automaticheskaya svarka 10:40–47
21. Skalskiy VR, Serghiyenko OM, Holaski L (1999) Generuvannya akustichnoyi emisiyi trischinami, scho rozvivayut'sya u zvarnich z'yednannyach (Generation of acoustic emission by cracks which develop in the welded joints). Tekhnichskaia diagnostika i nerazrushajuschii kontrol (Technical diagnostics and nondestructive testing) 4:23–31
22. Trufiakov VI (1991) Puti povysheniya nadezhnosti pri odnovremennom snizhenii metall-loemkosti svarnych konstrukziy (Ways of improvement of reliability with simultaneous decrease of specific content of metals of welded structures). Ibid 3:3–8
23. Troitskiy VA, Rad'ko VP, Demidko BG (1983) Defekty svarnych soedineniy i sredstva ich obnaruzheniya (Defects in welded joints and tools for their detection). Vyshcha shkola, Kiev
24. Nedosieka AYa (2001) Osnovy rascheta i diagnostiki svarnych konstrukziy (Basis for calculation and diagnostics of welded structures). Indprom, Kiev
25. Makarov EL (1981) Cholodnye treschiny pri svarke legirovannych staley (Cold cracks in of alloyed steels welding). Mashinostroyenie, Moskva
26. Smiyan OD (1985) Prognozirovanie obrazovaniya i razvitiya cholodnych treschin v konstrukzionnych materialach s pomosch'yu segregazionnych kart primesey vnedreniya

(Prediction of cold cracks initiation and propagation in structural materials with the use of segregation maps of interstitial impurities). Diagnostika i prognozirovanie razrusheniya svarnych konstrukziy (Diagnostika i prognozirovanie razrushenia svarnykh konstruktsii) 1:59–67
27. (1985) GOST 25.506–85. Raschety i ispytaniya na prochnost'. Metody mecha-nicheskich ispytaniy metallov. Opredelenie charakteristik treschino-stoykosti (vyazkosti razrusheniya) pri staticheskom nagruzhenii. Vved. v deystvie 27.03.1985g. (State Standard 25.506–85. Calculation and testing for strength. Methods of materials mechanical testing. Determination of crack growth resistance characteristics (fracture toughness). Implemented 27.03.1985). Izdatel'stvo standartov, Moskva
28. (1985) GOST 1497-84 Metally. Metody ispytaniy na rastyazhenie (Standard 1497-84. Metals. Methods of tensile testing). Izdatel'stvo standartov, Moskva
29. Skalskiy VR et al (1998) Pristroyi i ustanovki dlya vyznachennya trischynostiykosti konstrukziynych materialiv metodom akustychnoyi emisiyi (Equipment and devices for evaluation of crack growth resistance of structural materials by the method of the acoustic emission). Preprint, NAN Ukrayini, Fizyko-mechanichnyi institut, 1(1998), L'viv
30. Andreykiv AYe et al (1990) Metodicheskie aspekty primeneniya metoda akusticheskoy emissii pri opredelenii staticheskoy treschinostoykosti materialov (Methodical aspects of application of the acoustic emission method for evaluation of static crack growth resistance of materials). Preprint, NAN Ukrayini, Fizyko-mechanichnyi institut, 165(1990), L'viv
31. Lysak MV, Skalskiy VR (1997) Metodychniy pidkhid dlya eksperymental'noyi akustyko-emisiynoyi ozinky trischynotryvkosti konstrukziynych materialiv (Methodical approach for experimental acoustic emission evaluation of the crack growth resistance of structural materials). Fizyko-chimichna mechanika materialiv (Physicochem Mech Materi) 5:17–29
32. Pustovoi VM et al (1990) Vplyv nyz'kych temperatur na statychnu ta dynamichnu trischynostiykist' materialiv pidiymal'no-transportnych mechanizmiv (The effect of low temperatures on static and dynamic crack growth resistance of materials of lifting-transport mechanisms). Ibid 6:80–84
33. Skalsky VR (1996) Investigation of AE properties of the hoists. In: Panasyuk VV (ed) Advances in fracture resistance in materials. Tata McGraw-Hill Publishing Co. Ltd, New Delhi, pp 639–644
34. Andreikiv OY, Skalskyi VR, Lysak MV (1994) Sposib kontrolu rostu trischyn u zrazkakh materialiv (A method of checking the growth of cracks in the material specimens). Patent of Ukraine N2914, MPK: G01N29/14, Bul. 5-1, 26 Dec 1994
35. Greshnikov VA, Drobot YuB (1976) Akusticheskaya emissiya (Acoustic emission). Izdatel'stvo standartov, Moskva
36. Skalskiy VR et al (1998) Doslidzhennya za sygnalamy AE prozesiv ruynuvannya u konstrukziynych stalyach ASO (Researches of fracture processes in artillery infantry armament structural materials using the AE signals). In: Zbirnyk praz' II Mizhnar. konf. "Artyleryis'ki stvol'ni systemy, bojeprypasy, zasoby artyleryis'koyi rozvidky ta keruvannya vognem" (Proceedings of II international conference on "Artillery trunk systems, ammunitions, facilities of artillery reconnaissance and fire-control", Kiev, 27–29 Oct 1998)
37. Mykytyshyn SI, Hrytsyshyn PM (1981) Sposob mekhanicheskikh ispytaniy obraztsov na prochnost' (A method of mechanical strength testing of specimens). USSR Inventor's certificate, 879373, G01N3/00, Bul. No. 41, 07 Nov 1981
38. Andreykiv AY et al (1993) Spektral'nyy analiz signalov akusticheskoy emissii rastuschey treschiny (Spectral analysis of acoustic emission signals of a growing crack). Tekhnichskaia diagnostika i nerazrushajuschii kontrol (Tech Diagn Nondestr Test) 3:75–84
39. Climent FJ, Cribbs R, Eckert T (1968) Nondestructive testing and performance monitoring techniques (Updated instrumentation techniques for monitoring embankmens and concrete structures for civil works). In: Final report on contract SA N.o 157161 with the State of California, Department of Water Resources. Aerojet-General Corporation. Sacramento, California, Nov 1968

40. Li ST, Ramakrishnan V, Russell JE (1970) Where stands nondestructive testing of concrete and whither? Int J Nondest Testing 2:281–300
41. Muenow RA (1973) Large scale applications of acoustic emission. IEEE Trans Sonics and Ultrasonics 20(48):85–96
42. Sevall GW Jr (1973) Nondestructive testing of construction materials and operations. Champaign, Illinois
43. Galambos CF, McGorney CH Opportunities for NDT of highway structures. Mater Eval 33 (7):168–175
44. Hardy HR Jr, Belesky RM, Ge Maochen (1988) Acoustic emission/microseismic source location in geotechnical applications. In: Proceedings of 4th European conference, London, 13–17 Sept 1987, vol 2. Oxford, 1988, pp 3066–3075
45. Muenov RA (1974) Uses of acoustic emission in the construction industry. In: Proceedings of the second acoustic emission symposium, Tokyo, Japan, 2–4 Sept 1974
46. Eitzen DG, Wadley HNG (1984) Acoustic emission: establishing the fundamentals. J Res Nat Bureau Stand 89(1):75–100
47. Otsu M (1988) Acoustic emission control of concrete constructions. Konkurito kogaku 25 (12):5–11
48. Braginskii AP et al (1984) Akustikoemissionnoe obsledovanie zheleznodorozhnych mostov (Acoustic emission investigation of railroad bridges). In: Sbornik dokladov I Vsesoyuzn. konf. "Akusticheskaya emissiya materialov i konstrukziy" (Proceedings of the first all-union conference. " Acoustic emission of materials and constructions", Rostov-upon the-Don, 11–13 Sept 1984), vol 1. Rostov-na-Donu
49. Sakuda T et al (1988) Acoustic emission control of bridge reinforced concrete constructions. Khikhai kensa 37(9):866–965
50. Gong Z, Nybor EO, Oommen G (1992) Acoustic emission monitoring of steel railroad bridges. Mater Eval 50(7):883–887
51. Muravin GB, Yerminson AL (1984) Ispol'zovanie akusticheskoy emissii dlya kontrolya sostoyaniya zhelezobetonnych mostov (Usage of acoustic emission for testing the state of railroad bridges). In: Sbornik dokladov I Vsesoyuzn. konf. "Akusticheskaya emissiya materialov i konstrukziy" (Proceedings of first all-union conference. "Acoustic emission of materials and constructions", Rostov-upon the-Don, 1984), vol 2. Rostov-na-Donu
52. Chausov NG et al (1998) Ispol'zovanie metoda akusticheskoy emissii dlya ekspress–kontrolya razrusheniya betonov s dobavkami plastifikatorov (Usage of the method of acoustic emission for express-evaluation of fracture of concretes with plasticizers additives). Tekhnichskaia diagnostika i nerazrushajuschii kontrol (Tech Diagn Nondestr Test) 3:12–16
53. Makhonin AI et al (1984) Akustiko-emissionnaja diagnostika mostovykh i stroitel'nykh konstruktsij (Acoustic emission diagnostics of bridges and buildings). In: Ispol'zovanie metoda akusticheskoy emissii dlya ekspress—kontrolya razrusheniya betonov s dobavkami plastifikatorov (Proceedings of first all-union conference. "Acoustic emission of materials and constructions", Rostov-upon the-Don, 1984), vol 2. Rostov-na-Donu
54. Arrington M, Evans BM (1977) Acoustic emission testing of high alumina cement concrete. NDT Int 7:81–87
55. McClung RW (1972) On nondestructive testing in the USA of prestressed concrete pressure vessels for nuclear reactors. In: Nondestructive testing for reactor core components and pressure vessels, pp 527–540
56. Gorbunov IA et al (1984) Razrabotka i vnedrenie ekspress-metodov ozenki sostoyaniya nesuschich elementov krupnopanel'nych zdaniy na osnove statisticheskogo analiza i akusticheskoy emissii (Development and implementation of express-methods of evaluation of the state of large-panel structures using statistic analysis and acoustic emission). In: Ispol'zovanie metoda akusticheskoy emissii dlya ekspress–kontrolya razrusheniya betonov s dobavkami plastifikatorov (Proceedings of first all-union conference. "Acoustic emission of materials and constructions", Rostov-upon the-Don, 1984), vol 2. Rostov-na-Donu
57. Takao U et al (1992) AE waveform analysis for rock mass in grout injection of dam. Takenaka gijutsu kenkyu hokoku 47:61–71

58. Potapov AI et al (1993) Akustikoemissionnyy kontrol' nesuschey sposobnosti merzlych osnovaniy sooruzheniy i prinzipy postroeniya avtomatizirovannych diagnosticheskich sistem (The acoustic emission control of bearing capacity of frozen foundations of buildings and principles of construction of automated diagnostic systems). Defektoskopia 3:22–26
59. Muravin GB et al (1991) Metod akusticheskoy emissii v issledovaniyach podvizhki gruntov. (Obzor) (Method of acoustic emission in investigations of soils moving (a review)). Ibid 11:3–17
60. Lantukh-Liashchenko AI (1998) Problem of creation of the national system of bridges exploitation. In: Proceedings of Ukrainian scientific-practical interbranch seminar "modern problems of planning, building and exploitation of constructions on the roads". Kiev
61. Bondar' NG. (1986) Kak rabotayut mosty? (How do bridges work). Naukova dumka, Kiev
62. Vinogradskii DYu, Prudenko YuD, Shruratovskii AA (1985) Ekspluataziya i dolgovechnost' mostov (Operation and life time of bridges). Budivelnyk, Kiev
63. Strakhova NS (1992) Ekspluataziya ta rekonstrukziya mostiv (Exploitation and reconstruction of bridges). NMK VO, Kiev
64. Vasyliev AI, Polevko VP (1995) Dolgovechnost' zhelezobetonnych mostov i mery po uvelicheniyu sroka ich sluzhby (Life time of iron-concrete bridges and measures for improvement of their service life). Avtomobilnye dorogi 9:30–32
65. Koval PM (2003) Vikoristannya metodu akustychnoyi emisiyi pry doslidzhenni mostiv (Use of the acoustic emission method in investigation of bridges). Avtoshliakhovyk Ukrainy 1:34–37
66. Filonenko SF (1999) Akusticheskaya emissiya. Izmereniya, kontrol', diagnostika (Acoustic emission. Measuring, testing, diagnostics). KNUTCA, Kiev
67. Koval PM, Stashchuk PM, Fal AY (2003) Doslidzhennya prohonovoyi budovy novoho stalezalizobetonnoho avtodorozhn'ogo mosta z vykorystannyam metodu akustychnoi emisii (Research of a span structure of new steel iron-concrete motor bridge with the use of the acoustic emission method). Diagnostyka, dovgovichnist' ta rekonstrukziya mostiv i budivel'nych konstrukziy (Diagn Durab Reconstr Bridges Build Constr) 5:85–93
68. Koval PM et al (2003) Vivedennya z avariynoho stanu metalevoho mosta cherez riku Prut v m. Chernivzi (Getting out of metallic bridge across the Prut river in Chernivtsi from the emergency state). Ibid 5:72–84
69. Green A, Lockman C, Steek R (1964) Acoustic verification of structural integrity of polaris Chambers. Mod Plast, 137–139, 178, 180
70. Drouillard T (1979) Acoustic emission: a bibliography with abstracts. IFU/PLENUM, New York
71. Tatro CA, Liptai RG, Harris DO (1971) Acoustic emission technique in materials research. Int J Nondestr Testing 3(3):215–275
72. Shnaiderman IA (1974) Novye nerazrushayuschie metody kontrolya kachestva i technicheskoy diagnostiki. Obzor (New nondestructive methods for quality control and technical diagnostics. A review). Zarubezhnauya radioelectronika 5:74–82
73. Green JS, Toney BW (1972) Acoustic monitoring of airframe structural proof testing. J Environ Sci 15(1):20–23
74. Kishi T, Mori Y (1979) Evaluating the severity of rocket motor case during burst test using acoustic emission. In: Acoustic Emission Monitoring Pressurized Systems Ft Lauderdal, Fla, pp 131–148
75. Mashechkov VV, Muravin GB (1982) Akustiko emissionnyj sposob kontrolia izdelij sterzhnevoj i trubchtoj formy (Acoustic emission control method of products in the form of a rod and a pipe). USSR Inventor's certificate 905781, G01N29/04, Bul. No. 6
76. Green EJ, Rogers LM (1987) Location of discrete sources of acoustic emission in complex tubular joints. In: Non-destructive testing: proceedings of 4th European conference, London, 13–17 Sept 1987
77. Rapoport YM (1982) Sposob kontrolia kachestva izdelij (A test method for product quality). USSR Inventor's certificate 905777, G01N 29/04, Bull. No. 6
78. Zaretskii-Feoktistov GG, Rapoport YM (1982) Sposob opredelenija parametrov naibol'shego termocheskogo vozdejstvija perenesennogo izdeliem (A method for determination of

parameters of the largest thermal effect endured by a product). USSR Inventor's certificate 954875, G01 N29/04, Bul. No. 32
79. Andronov VM, Korshak VF, Kuznetsova RI, Nerubenko VV (1990) Sposob kontrolia narushenija sploshnosti pri termicheskom vozdejstvii na splavy (A method for integrity disturbance testing under thermal effect on alloys). USSR Inventor's certificate 1599758, G01N29/04, Bul. No. 38
80. Nechaiev YuA. (1982) Sposob nerazrushauschego kontrolia poverkhnostnykh defektov izdelij (A method for nondestructive testing of surface defects in products). USSR Inventor's certificate 911324, G01 N29/04, Bul. No. 9
81. Nakasa H (1980) Application of acoustic emission techniques to structural integrity assessment. In: Acoustic emission paper meet, Bad Nauheim, Apr 1979. Oberursel
82. Yamaguchi K, Oyaizu H (1988) Distributed fracture monitoring system by high speed processing of acoustic emission microdata. In: Non-destructive testing: Proceedings of 4th European conference, London, 13–17 Sept 1987, vol 4. Oxford
83. Tirbonod B, Hanacek L (1988) Some properties of acoustic emission signals measured in the vicinity of and crack during the cyclic pressure loading of and vessel. Ibid
84. Andreykiv OYe, Lysak NV (1989) Metod akusticheskoy emissii v issledovanii prozessov razrusheniya (A method of acoustic emission in investigation of fracture processes). Naukova Dumka, Kiev
85. Ohtsu M (1987) Determination of crack orientation by acoustic emission. Mater Eval 35 (9):1070–1075, 1082
86. McBride SL et al (1988) Acoustic emission detection of crack presence and crack advance during flight. Rep Progr Qnant Nondestract Eval 8B:1819–1825
87. Collacott RA (1989) Diagnostika povrezhdeniy (Diagnostics of Damages). Mir, Moskva
88. (2001) Rekomendazii schodo akustyko-emisiynoho kontrolyu ob'yektiv pidvyschenoyi nebezpeki. R 50.01-01. Vved.27. 01. 2001 r. (Recommendations on acoustic-emission testing of the highly dangerous objects. P 50.01-01. Introduced 27. 01. 2001)
89. (2003) Nazional'nyi standart Ukrayini DSTU 4227–2003. Nastanovy schodo provedennya akustyko-emisiynoho diagnostuvannya obyektiv pidvyschenoyi nebezpeki. Chynnnyi vid 2003 – 12 – 01 (National standard of Ukraine 4227–2003. Instructions on conducting acoustic emission diagnostics of the highly dangerous objects. Valid since 01 Dec 2003)